RI 9467

REPORT OF INVESTIGATIONS/1993

Improved 6.8-L Furnace for Measuring the Autoignition Temperatures of Dust Clouds

By Ronald S. Conti, Kenneth L. Cashdollar, and Richard A. Thomas

UNITED STATES DEPARTMENT OF THE INTERIOR

BUREAU OF MINES

Report of Investigations 9467

Improved 6.8-L Furnace for Measuring the Autoignition Temperatures of Dust Clouds

By Ronald S. Conti, Kenneth L. Cashdollar,
and Richard A. Thomas

UNITED STATES DEPARTMENT OF THE INTERIOR
Bruce Babbitt, Secretary

BUREAU OF MINES

Library of Congress Cataloging in Publication Data:

Conti, Ronald S.

Improved 6.8-L furnace for measuring the autoignition temperatures of dust clouds / by Ronald S. Conti, Kenneth L. Cashdollar, and Richard A. Thomas.

p. cm. — (Report of investigations; 9467)

Includes bibliographical references (p. 17).

1. Mine dusts. 2. Dust explosions. I. Cashdollar, Kenneth L. II. Thomas, Richard A. III. Title. IV. Series: Report of investigations (United States. Bureau of Mines); 9467.

TN23.U43 [TN312] 622 s—dc20 [622' .82] 92-35375 CIP

CONTENTS

ILLUSTRATIONS

TABLES

UNIT OF MEASURE ABBREVIATIONS USED IN THIS REPORT

atm	atmosphere	L	liter
cal/g	calorie per gram	m	meter
cm	centimeter	mil	thousandth of inch
cm^3	cubic centimeter	mL/kg	milliliter per kilogram
°C	degree Celsius	mm	millimeter
g	gram	ms	millisecond
g/m^3	gram per cubic meter	μm	micrometer
h	hour	s	second

IMPROVED 6.8-L FURNACE FOR MEASURING THE AUTOIGNITION TEMPERATURES OF DUST CLOUDS

By Ronald S. Conti,[1] Kenneth L. Cashdollar,[2] and Richard A. Thomas[3]

ABSTRACT

A new U.S. Bureau of Mines 6.8-L ignitability furnace was used to study the thermal autoignitability of dust clouds. This furnace has a quartz window to allow observation of the early stages of the ignition process and to allow measurement of the dust explosion temperature. Thermal ignitability data were obtained for various carbonaceous and metal dust clouds, with particular emphasis on various ranks of coal dusts.

One of the reasons for the construction of the new 6.8-L furnace was to evaluate the effect of chamber volume on the measured autoignition temperatures. Therefore, data from the 6.8-L furnace were compared with data measured earlier in a 1.2-L furnace. The conclusion is that the autoignition temperatures measured in the 6.8-L furnace were only slightly lower on average than those from the 1.2-L furnace.

These data on the minimum autoignition temperatures of various materials will be useful in analyzing the thermal ignition hazards of dust clouds in the mining industry and other industries that manufacture, process, or use combustible dusts.

[1]Electronics engineer.
[2]Research physicist.
[3]Physical science technician.
Pittsburgh Research Center, U.S. Bureau of Mines, Pittsburgh, PA.

INTRODUCTION

Dust explosions are a persistent hazard in the mining industry and in other industries such as plastics, chemicals, powdered metals, grains, cement, and electric power generation. For an explosion to occur, a flammable concentration of dust must be dispersed in air and an ignition source must be present simultaneously. Ignition sources may be characterized according to their type of energy source as electrical, chemical, or thermal. This U.S. Bureau of Mines report deals with a purely thermal source - a heated furnace into which a dust cloud is dispersed to determine the temperature at which the cloud will self-ignite. This temperature is called the spontaneous "autoignition temperature" (AIT) of the dust. The AIT of a dust is sometimes also called the "cloud ignition temperature." In either terminology, the word ignition refers to the generation of a self-sustained deflagration wave or explosion. It should be clearly distinguished from the "layer ignition temperature," which refers to the surface temperature at which a pile of dust in contact with a heated surface will undergo a self-sustaining heating. The exothermic heating within the layer or pile of dust will generate a smoldering mass or a fire (diffusion flame). The *layer* ignition temperature is often much lower than the *cloud* ignition temperature, and the final result of layer ignition is a much slower, mixing-limited, diffusion flame in which the heating occurs on a very long-time scale. The dust cloud ignition temperatures reported here are exclusively those that lead to deflagrations or explosions and should not be confused with the entirely different and less devastating ignition process that leads to a smoldering fire.

The minimum autoignition temperature (MAIT) is determined by tests over a range of dust cloud concentrations to determine the lowest temperature at which the cloud can self-ignite. The MAIT data can be used to prevent the accidental ignition of a dust cloud by limiting the temperature to which it is exposed. The MAIT data can also be used in conjunction with minimum electrical ignition energy data to evaluate the hazards from grinding and impact sparks (*1-2*).[4]

ACKNOWLEDGMENTS

The authors would like to acknowledge the valuable assistance of M. Hertzberg of the Pittsburgh Research Center during the design of the 6.8-L furnace. The authors also thank L. F. Miller and G. Radvansky, both formerly of the PRC, for their assistance in the early testing of the 6.8-L furnace.

PREVIOUS AUTOIGNITION FURNACES

GODBERT-GREENWALD FURNACE

Formerly, the Godbert-Greenwald furnace (*3-4*) was part of a variety of laboratory test equipment used for evaluating the explosibility of dust clouds. This furnace (fig. 1) consists of vertical tube made of aluminum oxide ceramic. The tube is 3.9 cm in diameter and 23 cm in length. Its volume is approximately 0.27 L. The top of the tube is connected by a glass adapter to a small brass chamber, with a hinged lid for inserting the dust. A solenoid valve between the dust chamber and an air dispersion tank (150 cm^3) controls the dispersion of the dust. The dust contained in the dispersion chamber is blown in through the top of the furnace. Ignition is indicated by the visual observation of flame coming through the open bottom. The data obtained from such experiments are now included in standard reference tables (*5*). Since the dispersed dust cloud is not completely confined within the furnace, its concentration is not accurately known, as noted in earlier publications (*6-7*). Two other problems associated with the open-bottom furnace are the short residence time for the dust in the high temperature zone and the uncertainty in the vertical temperature uniformity.

1.2-L IGNITABILITY FURNACE

The detailed structure of the Bureau's 1.2-L ignitability furnace (*7*) is shown in the vertical cross section in figure 2 and the perspective drawing in figure 3. The ceramic combustion chamber is made of magnesium aluminum silicate. It has an internal diameter of 10 cm and a volume of 1.2 L. It is wrapped with a 10-m length of Nichrome[5] heater wire. The combustion chamber is then surrounded by insulation. The 1.2-L furnace was designed

[4]Italicized numbers in parentheses refer to items in the list of references preceding the appendixes at the end of this report.

[5]Reference to specific products does not imply endorsement by the U.S. Bureau of Mines.

to correct for the dust dispersion uncertainty in the Godbert-Greenwald furnace, to improve on the visual criterion used to judge ignition, and to provide for more accurate control of the internal temperature. In addition to the descriptions here, further details of the 1.2-L furnace construction and test procedures are in references 7 through 10. Detailed machine drawings and fabrication procedures for the 1.2-L furnace are in appendix A.

There are four access holes through the outside wall of the furnace (figs. 2-3). One is used for a 12.5-mil (318-μm) Chromel-Alumel thermocouple located near the furnace wall. This thermocouple controls the initial or set temperature of the furnace. The temperature controller for the 1.2-L furnace was capable only of turning the voltage to the heating element on or off. It was not capable of varying the current, which would have resulted in a more stable furnace temperature. Another access hole is used for a 1-mil (25-μm) platinum-rhodium thermocouple in the center of the furnace. This fine thermocouple has a sufficiently fast time response to monitor the temperature of the dust-air mixture during ignition. The two remaining access ports in the side wall of the furnace may be used for spark electrodes (*7*, *9*) or for gas and dust sampling tubes (*11*). A fiberglass rupture diaphragm at the top of the furnace isolates the 1.2-L volume. The temperature distribution within the furnace, as measured by a thermocouple, is shown in figure 4. Data were measured at nominal temperatures of 200°, 500°, and 800° C. The temperature is uniform in the top part of the furnace, but decreases somewhat near the bottom.

The dust to be tested is placed in the disperser, which is manually inserted into the bottom part of the furnace only moments before the sequence of ignition test events is started. A 30-ms air dispersion pulse disperses the dust as it releases about 60 cm^3 of air at room temperature and atmospheric pressure from a pressurized reservoir into the furnace. Dust dispersion data published previously (*7*) have shown a uniform distribution of dust within the furnace. The time constant for heating the dispersed dust-air mixture to the initial temperature of the furnace is usually

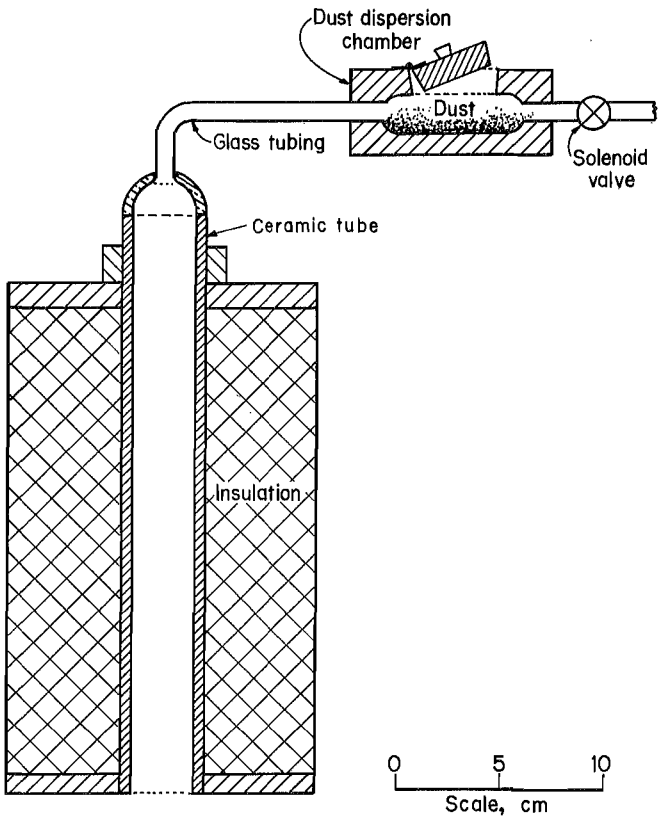

Figure 1.—Vertical cross section of 0.27-L Godbert-Greenwald furnace.

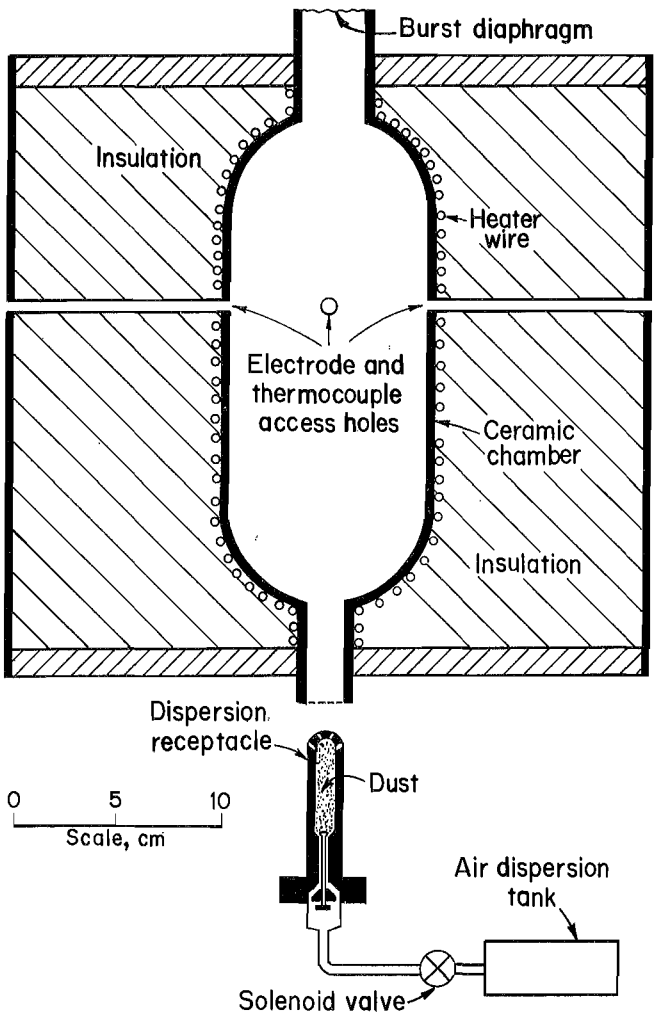

Figure 2.—Vertical cross section of 1.2-L ignitability furnace.

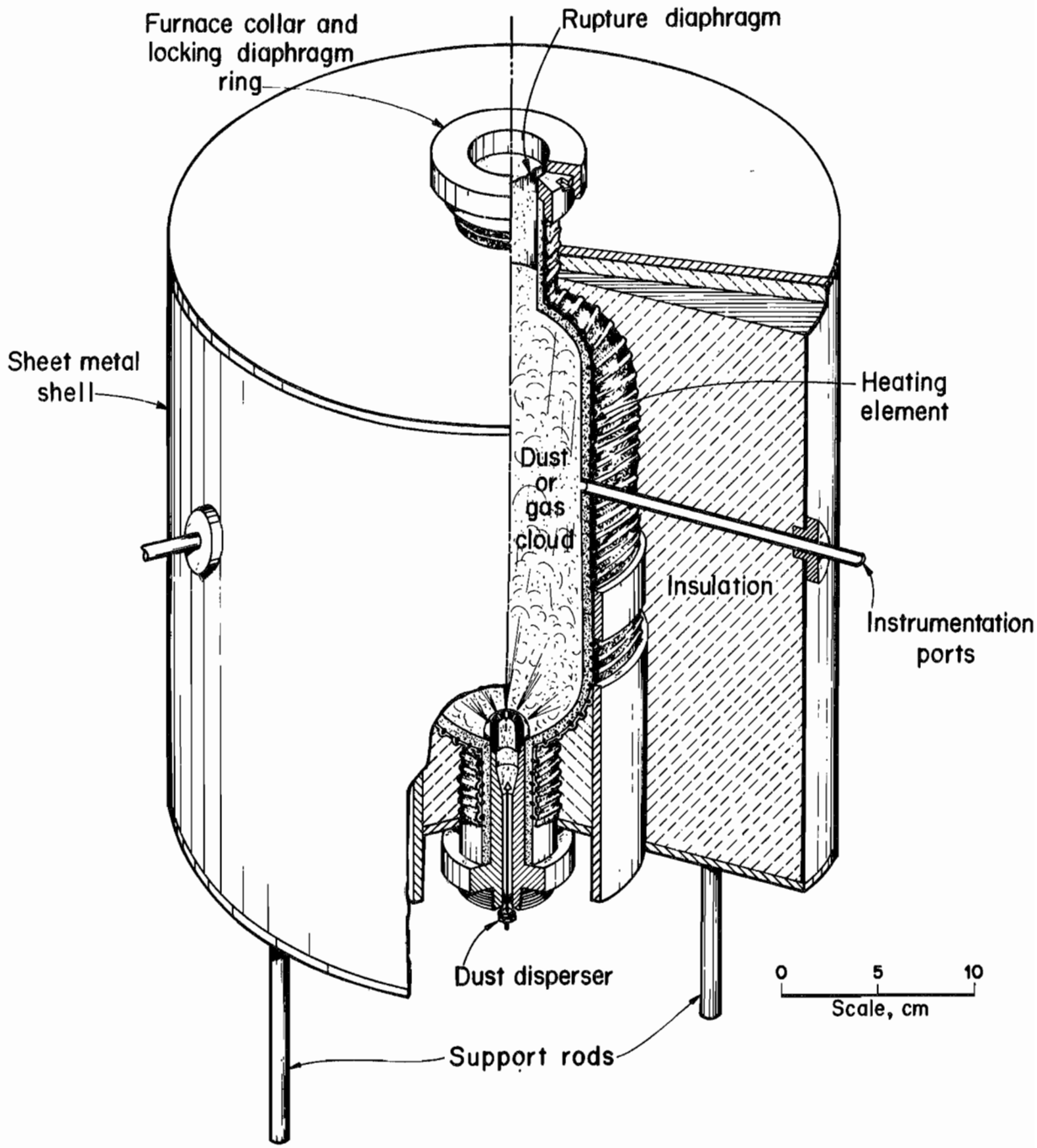

Figure 3.—Perspective schematic of 1.2-L ignitability furnace.

much shorter than the time constant for ignition, especially as one approaches the autoignition boundaries (*7*). Autoignition is accompanied by the rupture of the fiberglass diaphragm at an overpressure of 0.1 to 0.3 bar. The criterion for ignition is the rupture of the diaphragm with the simultaneous emission of flame from the top of the furnace within 3 s after dispersion. The time of flame emission is measured from the trace of the fine thermocouple. The criterion of ≤3 s that is used for the data in this report is somewhat longer than the criterion of ≤1.5 s that was used for some previous 1.2-L data (*10*). The earliest data reported from the 1.2-L furnace had only a qualitative time criterion (*7-9*).

Detailed measurements of the autoignition temperatures for several coals and other types of dusts have already been published (*7-10*). Data on the effect of particle size on the MAIT have also been published (*7-8, 10*). The MAIT values for methane and hydrogen gases have also been measured in the 1.2-L furnace (*12*). Interpretations of the MAIT data from the 1.2-L furnace are in references 10 and 13.

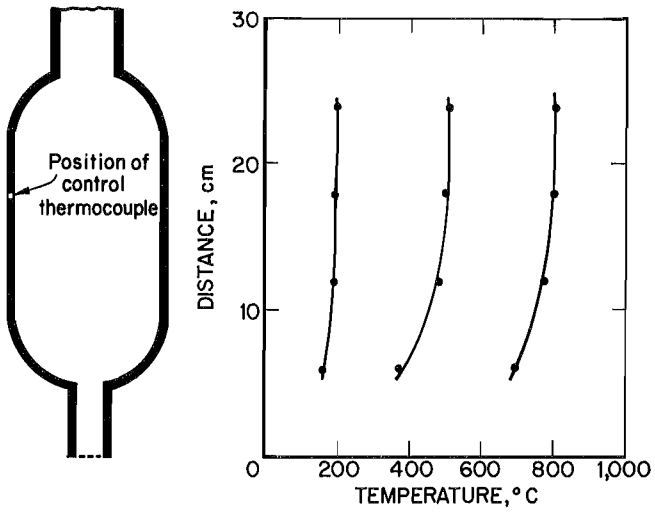

Figure 4.—Vertical temperature profile in 1.2-L furnace, measured at nominal temperatures of 200°, 500°, and 800° C.

NEW 6.8-L IGNITABILITY FURNACE AND EXPERIMENTAL PROCEDURES

The improved furnace system consists of a larger 6.8-L volume chamber, coupled to an automated dispersion system, enhanced vent mechanism, and an improved furnace temperature controller. A vertical cross section of the new 6.8-L furnace is shown in figure 5 and a perspective view is shown in figure 6. Detailed machine drawings and construction procedures of the 6.8-L furnace are in appendix B. An improved solid-state furnace controller and power supply allows for more precise control of the internal temperature of the new furnace. This is accomplished by varying the power factor. To increase the furnace temperature to the set value, the controller starts at full power. As the temperature of the furnace approaches the preset value, the power factor decreases to 3/4, 1/2, or 1/4. This technique eliminates excess temperature overshoot and maintains a constant furnace temperature. This is a major improvement over the 1.2-L furnace controller, which was only able to turn the voltage on or off.

The detailed structure of the Bureaus's 6.8-L ignitability furnace is shown in figures 5 and 6. The ceramic combustion chamber is made of magnesium aluminum silicate and has inside dimensions of 19.1 cm diameter and 44.5 cm overall height. The internal volume of 6.8 L is calculated with the disperser inserted into the furnace. Threads or grooves were machined on the outside of the ceramic chamber so that it could be wrapped with a 24-m length of 12-gauge Nichrome (80% Ni and 20% Cr) heater wire.[6] The axial temperature gradient within the furnace was reduced by concentrating the windings toward the ends. The heated chamber is insulated with a layer of ceramic, braided cloth. The outer covering consists of a cylindrical sheet metal shell that is 44.6 cm diameter by 39.8 cm high, with insulator boards (calcium silicate) at the top and bottom to hold the chamber in place. The remaining volume between the wrapped chamber and the metal shell is filled with several layers of ceramic blanket insulation to reduce heat losses.

Six access holes pass through the furnace walls. Two are used for thermocouples. A 12.5-mil (318-μm) Chromel-Alumel thermocouple located near the center axis of the furnace controls the furnace set temperature. A 1-mil (25-μm) platinum-rhodium thermocouple is positioned at the center axis of the furnace to observe rapid

[6]During some ignitions in the 6.8-L furnace, cracks developed on the interior walls of the ceramic chamber. This may have been due to a weakening of the chamber wall during the machining of the grooves for the heater wire. The cracks had to be repaired with high-temperature cement. A different design, such as molded rather than machined grooves, would probably improve the strength of the ceramic chamber.

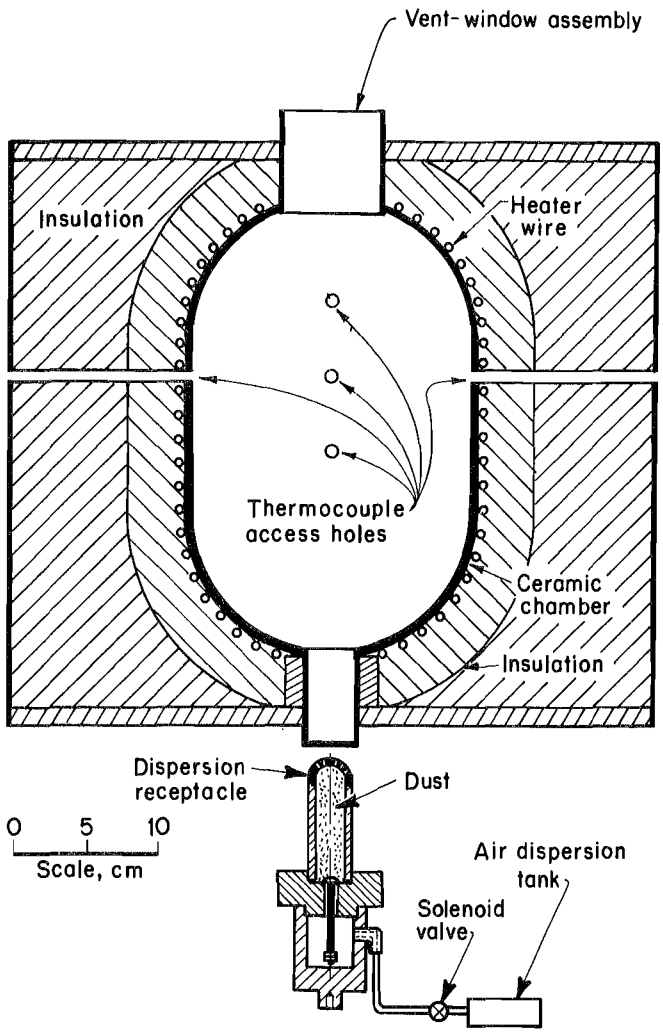

Figure 5.—Vertical cross section of 6.8-L ignitability furnace used to study thermal ignitability of dust clouds.

changes in the temperature of the dust-air mixture during ignition. The remaining four holes can be used for spark electrodes, a pressure transducer, or a rapid gas and dust sampling collection device (*11*).

The dust dispersion system was also improved. A detailed sketch of the brass dispersion system is shown in figure 7. The nozzle cap of the dust receptacle contains 34 small (1.6-mm-diameter) holes through which the dust is ejected as fine jets; this process breaks up dust agglomerates formed in the dispersion receptacle. The dust dispersion uniformity data will be presented later in this section. By interfacing a double-acting air-piston with the dust disperser, the operator is no longer required to manually insert the dust disperser receptacle into the bottom of the furnace. Once the predetermined mass of dust is loaded into the dust dispersion receptacle and the nozzle cap is replaced, activation of a foot switch automatically inserts the dust disperser into the base of the furnace. After 0.1-s delay, an air pulse automatically ejects the dust from the dispersion receptacle into the furnace. This short delay time minimizes the possible heating of the dust while it is still in the dispersion receptacle. The dust is dispersed by a 30-ms air pulse from a 175-cm^3 reservoir pressurized initially at 4.8 bar. The dispersion pulse releases about 340 cm^3 of room temperature, atmospheric pressure air into the furnace. After a preset time of 6 s, the dust receptacle is automatically retracted from the bottom of the furnace. The dispersed dust is exposed to the oven temperature for at least several seconds before the dust would settle by gravity.

The enhanced vent-window mechanism (fig. 6) replaces the previously used rupture diaphragm, which was a glass microfiber filter placed at the top of the 1.2-L furnace. The vent mechanism or door assembly consists of a hinged inconel furnace collar and a window flange. Inconel was chosen for its low expansion coefficient and corrosion resistance. The collar is fitted around the protruding portion of the top ceramic combustion tube and bolted to the top insulator board. The window flange assembly is hinged to the furnace collar. This allows the window to open for explosion venting during testing. It can also be opened manually for cleaning. The window is made of quartz and has the added protection of two ceramic paper gaskets to protect it from mechanical stress and thermal expansion. In normal operation, the vent-window assembly is closed to seal the furnace. If ignition of the dust cloud occurs during a test, the hinged window assembly opens, allowing the flame and hot gases to vent as shown in figure 8. The vent-window opens at an overpressure of 0.03 to 0.1 bar during ignitions in the 6.8-L furnace. Two keeper bars prevent the hinged window assembly from falling back onto the ceramic top after venting. Therefore, after a test, the assembly must be manually pushed back into its initial position. The quartz window provides an opportunity to take high-speed videos of the dust cloud ignition or to measure the radiation from the burning dust cloud.

In a 6.8-L thermal ignitability test, the criteria for ignition include both the opening of the vent-window assembly and the emission of flame from the top of the chamber (fig. 8). Both these criteria must occur within 6 s after dispersion, before the retraction of the dust disperser. A high percentage of the ignitions occur within 3 s of dispersion. The longer (6 s) time criterion is used for the

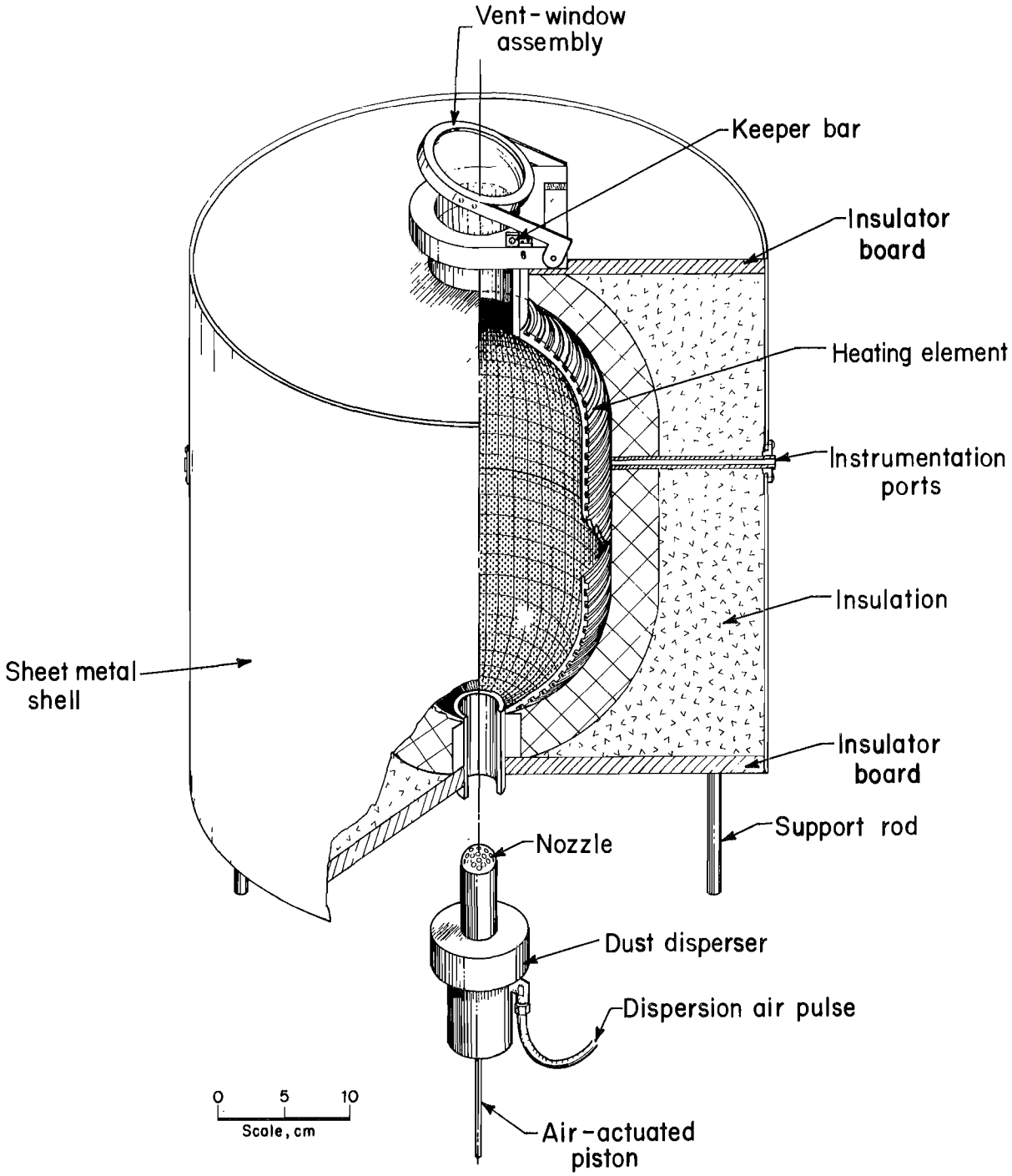

Figure 6.—Perspective schematic of 6.8-L ignitability furnace.

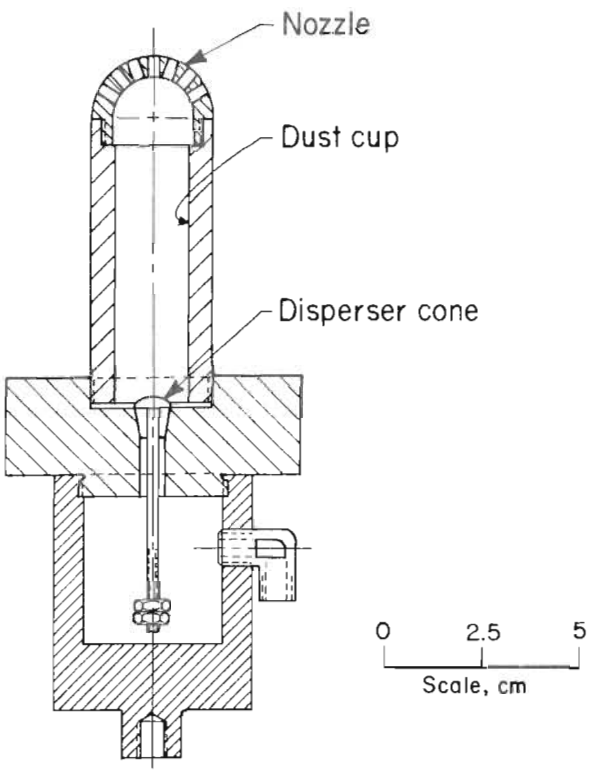

Figure 7.—Automated dispersion receptacle.

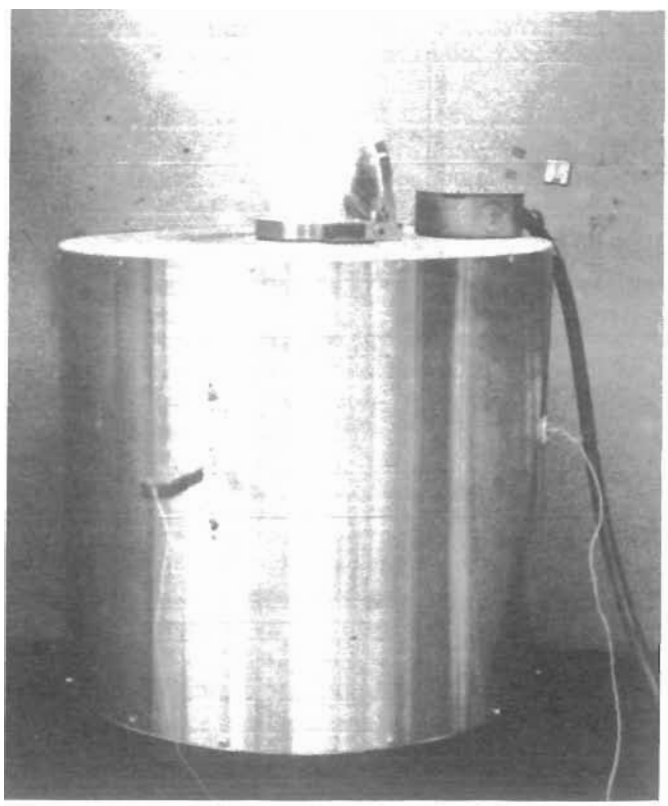

Figure 8.—Ignition of polyethylene dust cloud showing flame exiting top vent-window of 6.8-L furnace.

6.8-L furnace because its internal diameter is almost twice that of the 1.2-L furnace. It would, therefore, take longer for the flame to propagate and build up sufficient pressure to vent the 6.8-L furnace.

After a test, the vent-window is opened manually (if it was not already raised by the explosion) and an air blast through the furnace removes any remaining dust. At the end of a series of tests or after five consecutive nonignition tests, the furnace is heated for 1 h at 950° C to burn off any residual dust coating the walls of the furnace.

Data were obtained on the temperature distribution within the furnace by probing vertically along the furnace axis with a thermocouple and by probing radially at the furnace center with a thermocouple. The measured uniformity at four furnace temperatures is shown in figure 9. The data show a more uniform temperature in the 6.8-L furnace than in the 1.2-L furnace (fig. 4).

A miniature optical dust probe (*7, 14-15*) was used to measure the uniformity of the dust cloud and the effectiveness of the dispersion. The probe consists of a

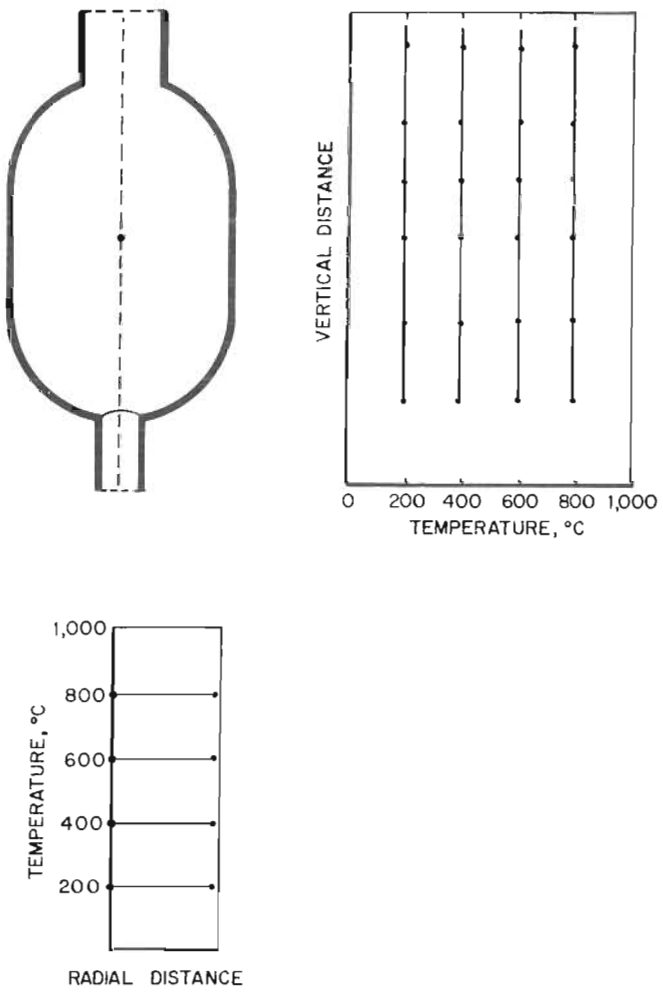

Figure 9.—Vertical and radial temperature profiles in 6.8-L ignitability furnace, measured at nominal temperatures of 200°, 400°, 600°, and 800° C.

light-emitting diode (LED) and a silicon photodetector that measures the transmission of light through a 1.8-cm path length in the dust cloud. Typical recorder traces for the optical dust probe are shown in figure 10. The dust used in these tests was Purple K, a fire extinguishant composed of potassium bicarbonate ($KHCO_3$) powder that is specially fluidized so that it readily disperses as single particles. Also, it does not significantly coat the LED and detector windows (*15*). Initially, before dust dispersion, there is no attenuation of the light source. After dispersion of the dust, the transmission rapidly reaches a given level determined by the mass concentration of the dust and its particle size. The trace at the top of figure 11 is for a Purple K concentration of 600 g/m^3 and the one at the bottom is for 1,200 g/m^3. As expected, the transmission is lower for the higher dust concentration. As can be seen from the traces, the dust remains suspended at a relatively constant concentration for a time scale on the order of seconds.

More detailed data on the uniformity of dispersion are shown in the semilogarithmic plot of figure 11, where transmission measurements were made along the furnace chamber axis at several heights from the chamber base. The dust probe transmission data show that the dispersed Purple K dust is uniform along the entire axis of the furnace. Ideally, the dust probe transmission data should obey the Bouguer-Beer-Lambert law, which is

$$\tau = \frac{I}{I_o} = \exp(-QnA\ell) = \exp\left[-\frac{3QC_m\ell}{2\rho D}\right]$$

where τ is the light transmission or ratio of the transmitted intensity I to incident intensity I_o, Q is a dimensionless extinction coefficient, n is the number density of particles, A is the cross-sectional area of a particle of diameter D, ℓ is the path length, C_m is the mass concentration of particles, and ρ is the density of the solid particle. (A detailed discussion of the theory and calibration of the dust probe is found in reference 15.) The concentration value plotted is the mass of dust loaded into the dispersion receptacle divided by the volume of the furnace. The data in figure 11 show that the dispersion system is effective in generating a uniform cloud of dust.

The data in figure 11 are for Purple K dust dispersed by an air pulse from a reservoir initially at 4.8 bar. During preliminary testing of the furnace, additional data were obtained for Purple K dust dispersed with a 6.9-bar air pulse. The data did not differ significantly from those in figure 12. Therefore, for the standard testing procedure, the lower air dispersion pressure (4.8 bar) was used to minimize the amount of air entering the furnace.

Figure 12 shows chamber pressure and temperature plotted versus time for various test conditions in the 6.8-L furnace. The pressures were measured with a strain gauge transducer and the temperatures were measured with the 25-μm thermocouple in the center of the furnace. Figure 12*A* shows data for the dispersion air pulse without any dust. The absolute pressure trace shows a slight rise as the air enters the furnace and a return to atmospheric pressure as some air leaks out. Clearly, although the volume of the furnace is well defined, the chamber is not perfectly sealed. The thermocouple trace shows a drop in temperature as the room temperature air enters the heated furnace. The furnace temperature returns to the 500° C set temperature within a few tenths of a second. Figure 12*B* shows data for a coal dust dispersion at a concentration of 400 g/m^3 into the furnace at 500° C. The thermocouple trace shows a greater drop in temperature as the coal and air enter the furnace, but the temperature

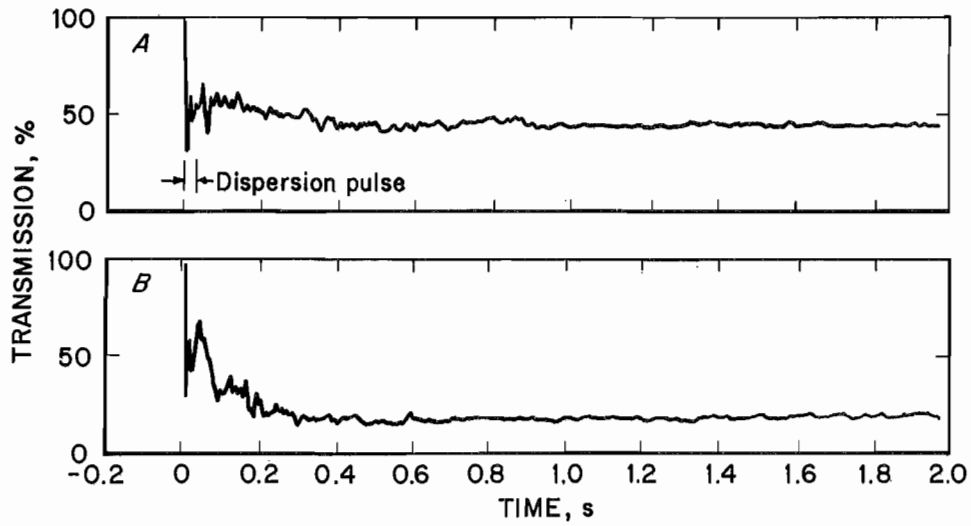

Figure 10.—Recorder traces of optical dust probe transmission in 6.8-L furnace at concentrations of 600 g/m^3 in *A* and 1,200 g/m^3 in *B*.

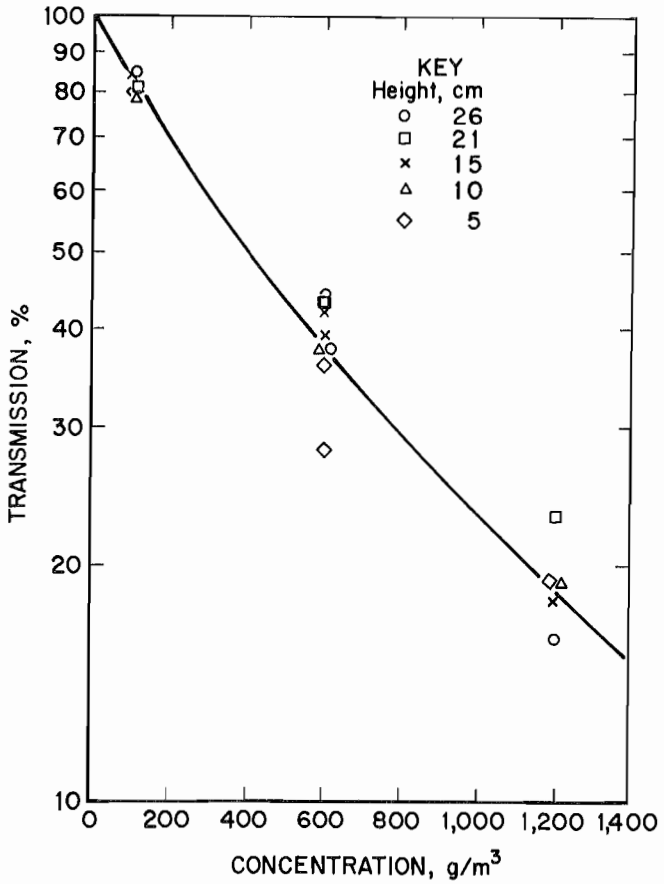

Figure 11.—Dust dispersion uniformity at five positions in 6.8-L ignitability furnace.

returns to the set value in about a second. The pressure trace now shows a drop in pressure due to the cooling effect as the larger mass of dust and air enters the furnace. The pressure quickly returns to atmospheric pressure as the dust and air are heated. For this test, the furnace set temperature of 500° C was below the autoignition temperature of the dust so there was no ignition. There was, however, a slight temperature rise above the set temperature of 500° C.

Figure 12*C* shows data for the same 400 g/m³ of coal dispersed into the furnace at a set temperature of 600° C. Again, the thermocouple trace shows a drop in temperature as the coal and air enter the furnace. However, after the temperature returns to the set temperature, there is a rapid temperature increase at a time of 1 s as the dust autoignites. At this same time, flame was observed exiting the top vent-window. Because of the venting, the temperature drops quickly as shown by the thermocouple trace. The pressure trace again shows a drop as the dust enters the furnace. This is followed quickly by a return to atmospheric pressure. Later, at a time of 1 s, there is a sharp increase in pressure at the time of ignition. The pressure quickly returns to atmospheric as the vent opens.

A more rapid ignition at a coal dust concentration of 200 g/m³ and a furnace set temperature of 700° C is shown in figure 12*D*. This time, the dust autoignites at a time of 0.3 s, even before the temperature has returned to the set value. As before, the temperature drops quickly as the flame is vented through the top vent-window.

Figures 12*A-D* represent the type of data that are collected in the 6.8-L furnace. For most of the tests, only the thermocouple was used. Data reported for each test would include a visual observation of flame or no flame. If there is flame, the time of ignition and the temperature rise are measured from the thermocouple trace. In a few cases, there is flame inside the furnace, but no flame ejecting through the vent-window. In this case, the thermocouple data are still recorded, but the test is not considered an ignition.

The Bureau's 6.8-L furnace has recently been included in the new American Society for Testing and Materials (ASTM) E1491 Standard Test Method for Minimum Autoignition Temperature of Dust Clouds. Other furnaces listed in this standard are the Godbert-Greenwald furnace, the Bureau's 1.2-L furnace, and the BAM oven (*16*).

THERMAL IGNITABILITY DATA IN 6.8-L FURNACE

The size analyses of the carbonaceous, agricultural, and chemical dusts tested in the 6.8-L furnace are listed in table 1. The order of the dusts in the table is based on their MAIT values, to be discussed later in this section. The oil shale was mined in Colorado and has a Fischer (*17*) oil assay of about 140 mL/kg. The gilsonite is a mined, asphaltic material from Utah. The first bituminous coal is from the Pittsburgh Seam; this dust has been used for decades as a standard test dust at the Bureau (*18*). The second two bituminous coals are from the Pocahontas Seam. The anthracite coal is from eastern Pennsylvania. The graphites are synthetically generated carbon. The two graphites are flakes, but the size analyses listed are based on equivalent spherical diameters, rather than the flake diameter or thickness. The lycopodium is a natural plant spore with a very narrow size distribution. It is often used

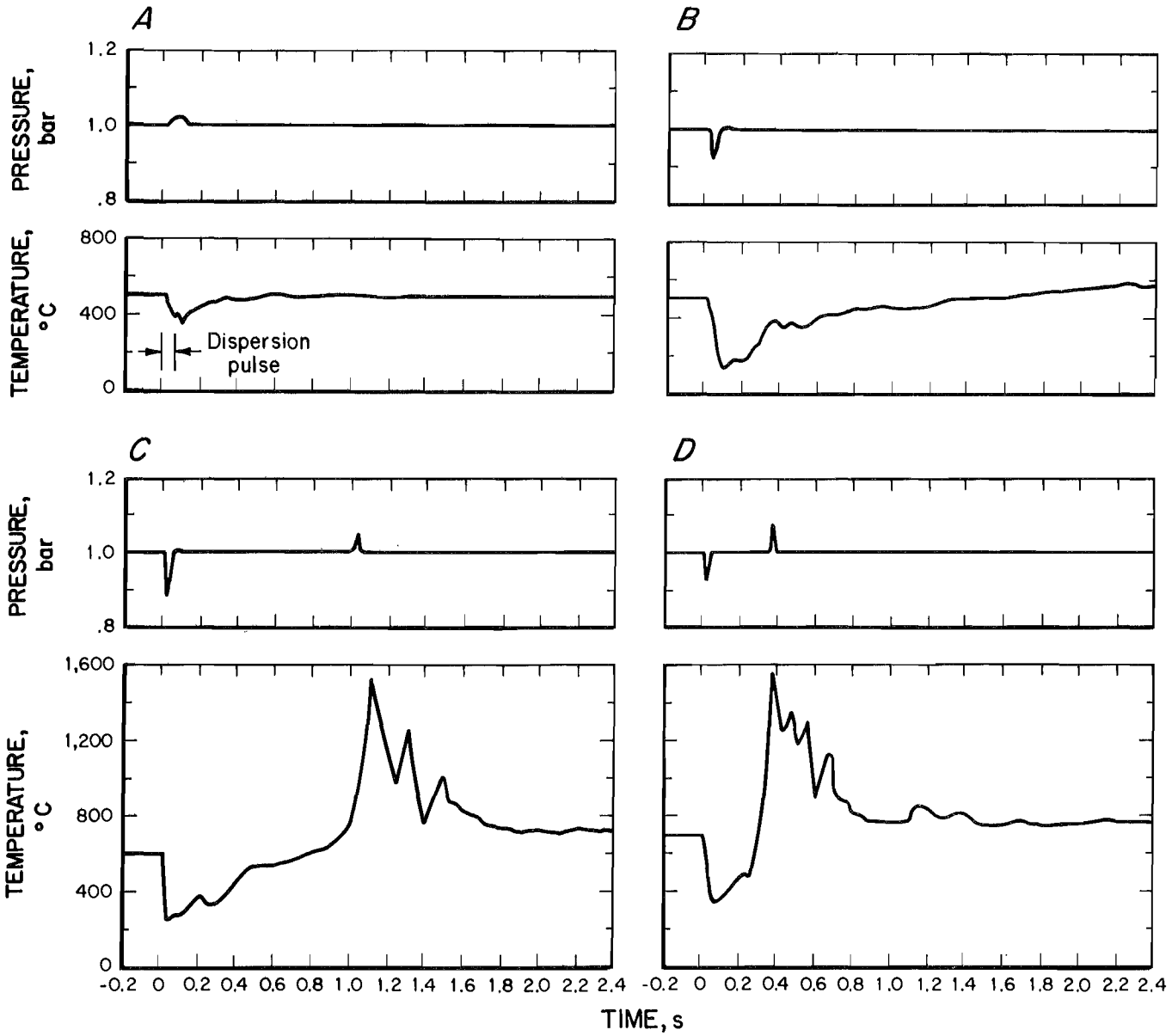

Figure 12.—Temperature and pressure traces: *A*, Dispersion air pulse at furnace temperature of 500° C; *B*, nonignition of coal dust cloud at 400 g/m^3 and 500° C; *C*, ignition of coal dust cloud at 400 g/m^3 and 600° C; *D*, rapid ignition of coal dust cloud at 200 g/m^3 and 700° C.

as a standard dust for ignitability and flammability testing (*9*). The cornstarch is a flammable dust from the agricultural industry. The sulfur, polyethylene $[(CH_2)_n]$, and anthraquinone $[C_{14}H_8O_2]$ are dusts from the chemical industry. The size distributions of these dusts were determined from a combination of sonic sieving data and Coulter counter data. In the Coulter (*19*) analyses (of the minus 200 mesh fraction of the dust), the particles are dispersed in isopropyl alcohol. The combined sieving and Coulter results are listed in columns 2 through 6 of table 1. The second and third columns list the weight percent of each dust that is less than 20 or 75 μm, respectively. The mass median particle diameter, D_{med}, is listed in the fourth column. In the fifth and sixth columns, $\bar{D}_w$ is the arithmetic volume or mass mean diameter and $\bar{D}_s$ is the arithmetic surface mean diameter. In the seventh

column, $\bar{D}_s$ is determined by a different method. As described in the previous section, optical dust probes can be used to measure the transmission through a dust cloud. Although the miniature dust probe was not used routinely in the 6.8-L furnace, most of these same dusts have also been dispersed in a 20-L explosibility test chamber (*18, 20*) that routinely uses one or two optical dust probes of a more advanced design (*14-15, 21*). Using the dust dispersion data from the 20-L chamber, equation 1 can be used to calculate the $\bar{D}_s$ values of the dusts, and the results are listed as $\bar{D}_s(\%\tau)$ in column 7 of the table. If the dusts agglomerate, the $\bar{D}_s(\%\tau)$ data can be larger than the $\bar{D}_s$ values in column six.

Table 1.—Size analyses of carbonaceous, agricultural, and chemical dusts

Dust	Amount, %		Diameter, μm			
	<20 μm	<75 μm	D_{med}	$\bar{D}_w$	$\bar{D}_s$	$\bar{D}_s(\%\tau)$
CARBONACEOUS						
Oil shale	49	75	19	53	12	11- 18
Gilsonite	36	91	28	37	19	14- 21
Bituminous coal:						
Pittsburgh	16	81	45	50	30	24- 45
Pocahontas-1	40	86	27	41	17	10- 15
Pocahontas-2	10	68	58	63	40	20- 40
Anthracite coal	23	85	40	45	24	13- 23
Graphite-1	100	100	1	2	1	3- 6
Graphite-2	~98	~100	~7	~8	~5	NA
AGRICULTURAL						
Lycopodium	1	100	28	28	26	70-150
Cornstarch	68	94	16	26	15	NA
CHEMICAL						
Sulfur	12	81	38	55	34	NA
Polyethylene	18	98	29	31	26	~70-180
Anthraquinone	2	73	56	62	50	27- 44

NA Not analyzed.

The size analyses of the metal dusts are listed in table 2. The order of dusts in the table is based on their MAIT values. Because of the much higher densities of the metal dusts, they cannot be accurately analyzed in the Coulter counter. Therefore, the precise size distributions cannot be determined for the metal dusts. All the metal dusts were 100% less than 75 μm (passing through a 200 mesh sieve). Column 2 lists the size range of the dusts as determined from scanning electron microscope (SEM) photographs. The $\bar{D}_s(\%\tau)$ values determined from optical dust probe data from the 20-L chamber are listed in column 3.

The proximate analyses (ASTM standard D3172) and heating values (ASTM standards D1989 and D2015) of the carbonaceous dusts are listed in table 3, in the same order as in table 1. Of the mined carbonaceous dusts, the gilsonite has the highest volatility, the Pittsburgh and Pocahontas bituminous coals are of intermediate volatility, and the anthracite has the lowest volatility. The graphite is essentially pure carbon with negligible volatility. The volatility for the oil shale is the sum of the oil and gas amounts from the Fischer assay as described in reference 22.

Table 2.—Size analyses of metal dusts

Dust[1]	SEM size range, μm	$\bar{D}_s(\%\tau)$, μm
Iron-1	2- 8	4- 6
Iron-2	10-80	~40-200
Tungsten	<1	1- 2
Tin	4-25	NA

NA Not analyzed.
[1]All were 100% minus 200 mesh (<75μm).

Table 3.—Chemical analyses of carbonaceous, agricultural, and chemical dusts

Dust	Proximate analyses, %				Heating value, cal/g
	Moisture	Volatiles	Fixed carbon	Ash	
CARBONACEOUS					
Oil Shale	1	15	NA	NA	1,780
Gilsonite	1	84	15	0	9,900
Pittsburgh coal	1	37	56	6	7,700
Pocahontas coal	1	17	76	6	8,100
Anthracite coal	2	8	79	11	7,150
Graphite	0	1	98	1	7,770
AGRICULTURAL					
Lycopodium	3	92	4	1	7,500
Cornstarch	12	85	3	0	3,680
CHEMICAL					
Sulfur	0	100	0	0	NA
Polyethylene	0	100	0	0	11,100
Anthraquinone	0	100	0	0	7,400

NA Not analyzed.

As an example of data from the 6.8-L furnace thermal ignitability tests, the results for Pittsburgh coal are shown in figure 13. The 6.8-L tests resulting in ignitions (solid circles) and nonignitions (open circles) are plotted on a graph of furnace temperature versus dust concentration. The solid curve shows the boundary between the upper region that is thermally ignitable in the 6.8-L furnace and the lower, nonignitable region. Also shown in figure 13 is the dashed line showing the same thermal ignition boundary as measured in the 1.2-L furnace (*7-10*). The MAIT measured for the Pittsburgh coal in the 6.8-L furnace is

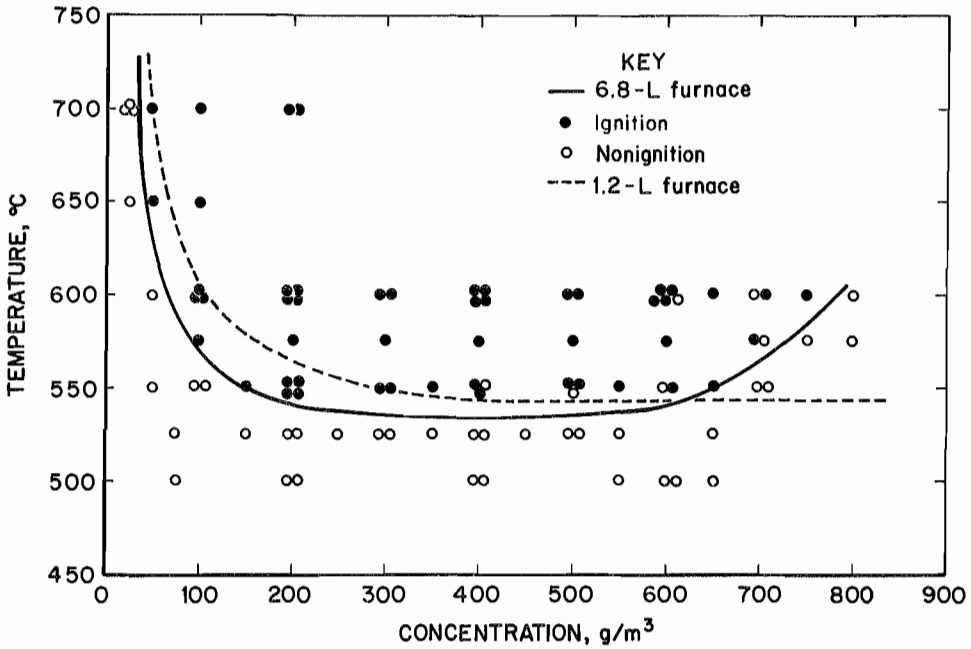

Figure 13.—Thermal ignitability data points (● and ○) and solid curve for Pittsburgh bituminous coal in 6.8-L furnace, compared with dashed curve for 1.2-L furnace.

530° C, slightly lower than the 540° C measured in the 1.2-L furnace. The general forms of the two curves are similar, as expected. At low dust concentrations, there is insufficient dust to have an explosion, even at high temperatures (*7-10*). Over the concentration region from 200 to 600 g/m^3, the 6.8-L data curve is rather flat. This is the part of the thermal ignitability boundary that defines the MAIT. At higher concentrations, the 6.8-L data curve rises as the dust becomes more difficult to ignite. The 1.2-L data curve remains flat out to higher concentrations. This difference at very high concentrations is probably related to the difference in chamber volumes and the way this affects the heating of the dust clouds. The lower surface to volume ratio of the 6.8-L furnace increases the time to heat the dust cloud after it has been dispersed into the furnace. The heating times can be seen in the thermocouple traces of figure 12*B-D*.

The 6.8-L thermal ignitability data for polyethylene are shown in figure 14. The AIT curve (solid line) corresponds to a boundary where one-third to one-half of the tests result in ignition. The general shape of the AIT curve is similar to that for the coal, but the polyethylene ignites at lower temperatures than the coal did in figure 13. Again, the data show a lower MAIT value in the 6.8-L furnace compared to the dashed curve for the 1.2-L furnace.

The Pittsburgh coal data in figure 13 were accumulated during four series of tests over a period of 18 months. The MAIT was the same for the coal in each of the test series. The polyethylene data in figure 14 were accumulated during three series of tests over a period of 20 months. The MAIT values for each of the series agreed to within 10° C. This shows good repeatability of the data from the 6.8-L furnace over a long period.

During preliminary testing of the 6.8-L furnace, AIT data for Pittsburgh coal and polyethylene were also obtained using an air dispersion pulse at the higher pressure of 6.9 bar, in addition to the standard dispersion pressure of 4.8 bar used for the data in figures 13 and 14. There was no observable difference in the MAIT for the coal under the two test procedures. For the polyethylene, the MAIT was slightly lower using the lower dispersion pressure. This was additional justification for using the 4.8 bar dispersion pressure as the standard test procedure.

The thermal ignitability data for lycopodium (using the standard test procedure) are shown in figure 15. For this dust, the MAIT value is 380° C in the 6.8-L furnace, significantly lower than the 440° C in the 1.2-L furnace.

A summary of the MAIT data from the 6.8-L furnace for various dusts is listed in table 4, where they are compared with earlier 1.2-L data. The dusts in the table are in order of their MAIT values in the 6.8-L furnace. If there is more than one size for a dust, it is listed in the table according to the MAIT value of the finest size. The MAIT value for a dust corresponds to the temperature at which one-third to one-half of the tests result in ignitions.

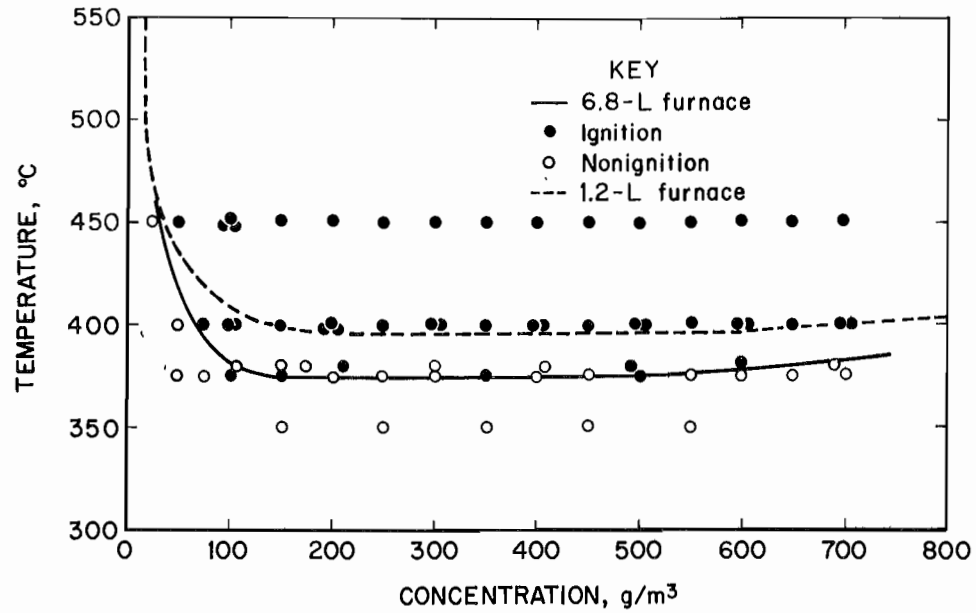

Figure 14.—Thermal ignitability data points (● and ○) and solid curve for polyethylene in 6.8-L furnace, compared with dashed curve for 1.2-L furnace.

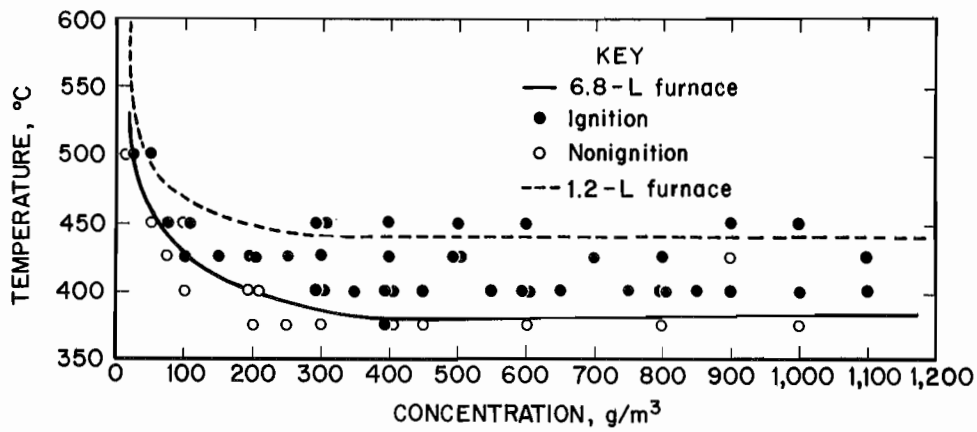

Figure 15.—Thermal ignitability data points (● and ○) and solid curve for lycopodium in 6.8-L furnace, compared with dashed curve for 1.2-L furnace.

For some of the dusts, there were no 1.2-L data. Also, the 1.2-L data from references 7 through 10 have been revised slightly for the table, based on the criterion of flame out of the furnace within 3 s. The earlier data sometimes used a criterion of 1.5 s or sometimes used only a qualitative time criterion. For most dusts, the revised MAIT values did not differ significantly from those in the earlier publications. The ignition criterion for the 6.8-L furnace is flame out of the top of the furnace within 6 s. The MAIT data denoted with the approximate symbols are those for which the data were less repeatable than normal or for which there were only a few ignition tests.

In comparing the 1.2- and 6.8-L data, there does not appear to be any large systematic difference in the MAIT values for the two furnace sizes. On average, the MAIT values in the 6.8-L furnace are slightly lower, but most of the MAIT data agree to within 30° C between the two furnaces. The only large difference is for the lycopodium, where the MAIT in the 6.8-L furnace is 60° C lower than in the 1.2-L furnace. MAIT data for the 1.2-L furnace were previously compared with those from the Godbert-Greenwald furnace and BAM oven in references 7 and 10.

Table 4.—Comparison of dust cloud minimum autoignition temperatures (in °C) measured in 1.2-L and 6.8-L furnaces

Dust	1.2-L furnace	6.8-L furnace
CARBONACEOUS		
Oil Shale	490	480
Gilsonite	~470	500
Bituminous coal:		
Pittsburgh	~540	530
Pocahontas-1	~600	580
Pocahontas-2	NA	600
Anthracite coal	760	730
Graphite-1	820	830
Graphite-2	920	960
AGRICULTURAL		
Lycopodium	440	380
Cornstarch	390	390
CHEMICAL		
Sulfur	290	260
Polyethylene	390	370
Anthraquinone	≤680	~680
METALS		
Iron-1	NA	390
Iron-2	NA	640
Tungsten	NA	460
Tin	NA	740

NA Not available.

The first group of dusts in table 4 are characterized by a decreasing volatility and increasing fixed carbon content from gilsonite through graphite. The MAIT's for this group increase as the volatility decreases. Hertzberg (*13*) explains this inverse correlation in terms of the onset temperature for significant pyrolysis and devolatilization. Each of the dusts has a temperature at which sufficient volatiles are generated so that they can be ignited thermally; this temperature is the onset temperature. The higher volatile dusts in this first group appear to have lower onset temperatures, and the lower volatile dusts appear to have higher onset temperatures.

The oil shale dust is comprised of a kerogen matrix from which the combustible volatiles are generated and an inert shale component (*22-23*). For the oil shale, sufficient volatiles for ignition appear to be generated from the kerogen at a relatively low temperature. The lycopodium and cornstarch both come from living plants and have similar MAIT values. It was difficult to measure the MAIT for the anthraquinone in either of the two furnaces because the MAIT was found over a very narrow concentration range. This was in marked contrast to most of the dusts for which the AIT is flat over a wide concentration range as in figures 13 through 15. The sulfur dust had the lowest MAIT values of any of the dusts tested in either the 1.2- or 6.8-L furnace.

The last four dusts in table 4 are metals. Since the amount of vapor or volatiles generated from these metals is very low at these temperatures, these dusts may be igniting through reactions at the particle surfaces.

HIGH-SPEED VIDEO RECORDINGS OF THERMAL IGNITIONS

Direct observation of the early stages of the thermal ignition process was possible with the use of a high-speed video camera and the new vent-window assembly. The video camera recorded at 200 frames per second. Using two mirrors placed at specific angles above the vent-window, the video camera was able to record the dust ignition inside the furnace. The view was from the top of the furnace looking down towards the dust disperser. The video camera recorded the insertion of the dust disperser into the furnace, the dispersion of the dust, and the ignition of the dust cloud. Several dust ignitions were recorded, including polyethylene, Pittsburgh coal, and iron. All the video observations showed the same sequence of events. After the dust was dispersed, the particles would start to ignite at some point near the furnace wall. The flame would then propagate across the center of the furnace, igniting the remainder of the particles. Figure 16 shows frames from the video camera for ignition of a 200-g/m^3 coal dust cloud at a temperature of 550° C in the 6.8-L furnace. Frame A of the figure shows a view through the top of the furnace looking down toward the disperser before the injection of the dust. Frame B shows the first appearance of flame after ignition near the wall of the furnace. Rapid flame propagation across the furnace is shown in frames C, D, and E. By frame F, the flame has completely filled the furnace, and the window starts to lift. Later, frames showed the flame venting through the top of the furnace. The dusts ignited at various positions near the furnace wall during multiple tests. This confirms the temperature uniformity of the furnace wall.

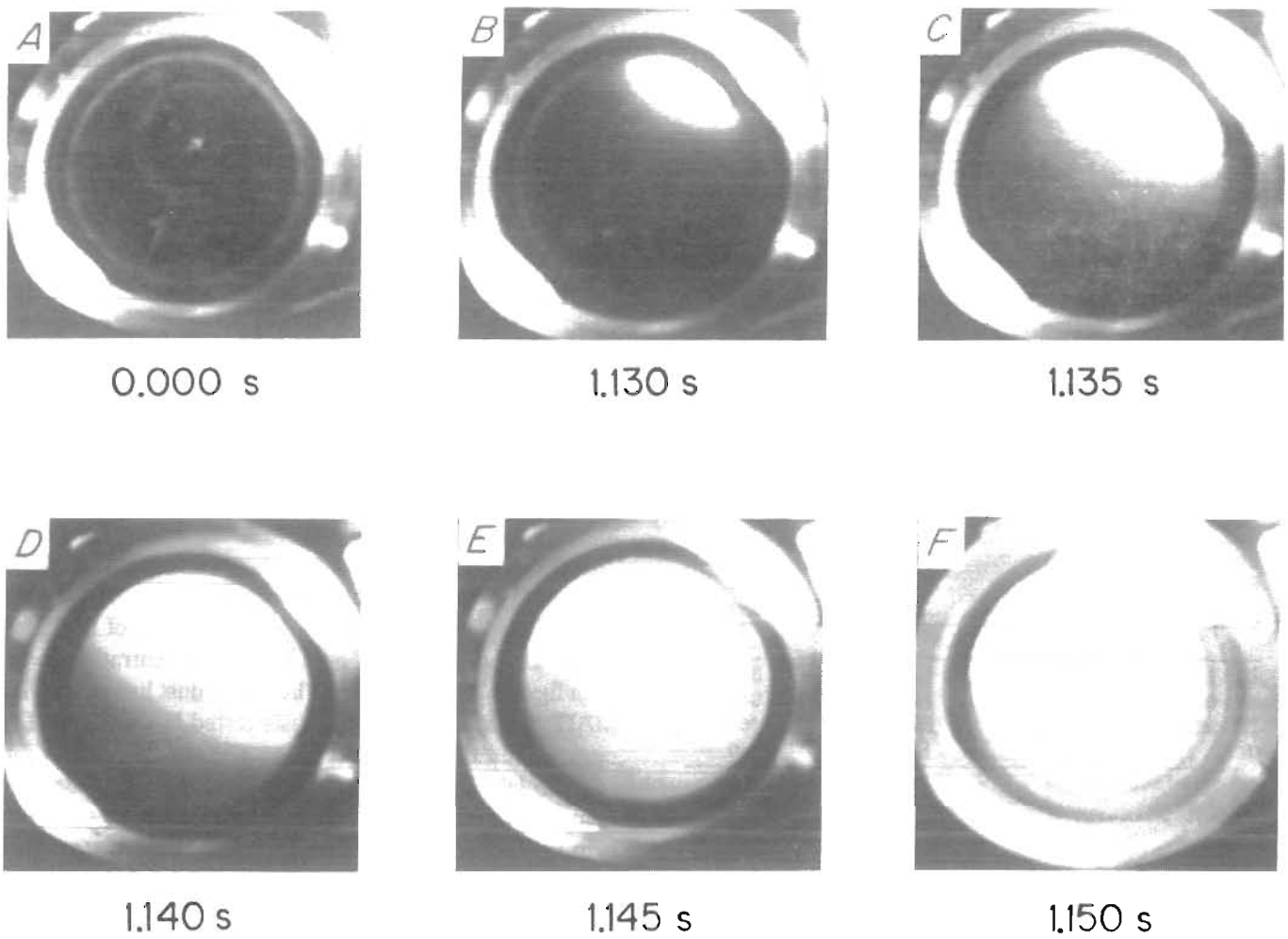

Figure 16.—Frames from high-speed video recording of ignition of 200-g/m^3 coal dust cloud at 550° C in 6.8-L furnace.

CONCLUSIONS

One of the reasons that the 6.8-L furnace was designed was to evaluate the effect of chamber volume on the measured MAIT data by comparing them to those from the 1.2-L furnace. In theory, the MAIT values might be lower in a larger volume chamber because of lower heat losses to the walls after the dust ignites. However, the lower surface to volume ratio in the larger furnace also increases the time to heat a dust cloud after it has been dispersed into the furnace. This would make it more difficult to ignite a dust in the larger furnace. On average, the MAIT data from the 6.8-L furnace are slightly lower than those from the 1.2-L furnace, but most of the MAIT data from the two furnaces agree to within 30° C. Based on this data for the 1.2-L and 6.8-L furnaces, the chamber volume has only a slight effect on the measured MAIT values. However, industrial volumes may be much larger than those of the laboratory furnaces tested here. Therefore, a large safety factor should always be used when applying the laboratory MAIT data to practical use.

REFERENCES

1. Bartknecht, W. Preventive and Design Measures for Protection Against Dust Explosions. Paper in Industrial Dust Explosions. ASTM STP 958, K. L. Cashdollar and M. Hertzberg, eds., Am. Soc. Test. Mater., Philadelphia, PA, 1987, pp. 158-190.

2. ____. Dust Explosions: Course, Prevention, Protection. Springer, New York, 1989, 270 pp.

3. Godbert, A. L., and H. P. Greenwald. Laboratory Studies of the Inflammability of Coal Dusts: Effect of Fineness of Coal and Inert Dusts on the Inflammability of Coal Dusts. BuMines B 389, 1935, 29 pp.

4. Dorsett, H. G., Jr., M. Jacobson, J. Nagy, and R. P. Williams. Laboratory Equipment and Test Procedures for Evaluating Explosibility of Dusts. BuMines RI 5624, 1960, 21 pp.

5. National Fire Protection Association (Boston, MA). Fire Protection Handbook. 17th ed., 1991, pp. 3-133 - 3-142.

6. Nagy, J., and J. Surincik. Thermal Phenomena During Ignition of a Heated Dust Dispersion. BuMines RI 6811, 1966, 25 pp.

7. Conti, R. S., K. L. Cashdollar, M. Hertzberg, and I. Liebman. Thermal and Electrical Ignitability of Dust Clouds. BuMines RI 8798, 1983, 40 pp.

8. Hertzberg, M., K. L. Cashdollar, D. L. Ng, and R. S. Conti. Domains of Flammability and Thermal Ignitability for Pulverized Coals and Other Dusts. Paper in Nineteenth Symposium (International) on Combustion. Combust. Inst., Pittsburgh, PA, 1983, pp. 1169-1180.

9. Hertzberg, M., R. S. Conti, and K. L. Cashdollar. Electrical Ignition Energies and Thermal Autoignition Temperatures for Evaluating Explosion Hazards of Dusts. BuMines RI 8988, 1985, 41 pp.

10. Conti, R. S., and M. Hertzberg. Thermal Autoignition Temperatures From the 1.2-L Furnace and Their Use in Evaluating the Explosion Potential of Dusts. Paper in Industrial Dust Explosions. ASTM STP 958, K. L. Cashdollar and M. Hertzberg, eds., Am. Soc. Test. Mater., Philadelphia, PA, 1987, pp. 45-59.

11. Conti, R. S., M. Hertzberg, F. T. Duda, and K. L. Cashdollar. Rapid Sampling System for Dusts and Gases. Rev. Sci. Instrum., v. 54, 1983, pp. 32-36.

12. Conti, R. S., and M. Hertzberg. Thermal Autoignition Temperatures for Hydrogen-Air and Methane-Air Mixtures. J. Fire Sci., v. 6, 1988, pp. 348-355.

13. Hertzberg, M. Autoignition Temperatures for Coal Particles Dispersed in Air. Fuel, v. 70, 1991, pp. 1115-1123.

14. Liebman, I., K. L. Cashdollar, and R. S. Conti. Dust Cloud Concentration Probe. Rev. Sci. Instrum., v. 48, 1977, pp. 1314-1316.

15. Cashdollar, K. L., I. Liebman, and R. S. Conti. Three Bureau of Mines Optical Dust Probes. BuMines RI 8542, 1981, 26 pp.

16. Hattwig, M. Explosion Hazard Classification, Explosion Safety Parameters, and Relevant Measurement Techniques Applied in the Federal Republic of Germany. Paper in Proceedings of the International Symposium on the Explosion Hazard Classification of Vapors, Gases, and Dusts. Publ. NMAB-447, Natl. Acad. Press, 1987, pp. 159-179.

17. Stanfield, K. E., and I. C. Frost. Method of Assaying Oil Shale by a Modified Fischer Retort Test. BuMines RI 4477, 1949, 13 pp.

18. Cashdollar, K. L., M. J. Sapko, E. S. Weiss, and M. Hertzberg. Laboratory and Mine Dust Explosion Research at the Bureau of Mines. Paper in Industrial Dust Explosions, ASTM STP 958, K. L. Cashdollar and M. Hertzberg, eds., Am. Soc. Test. Mater., Philadelphia, PA, 1987, pp. 107-123.

19. Berg, R. H. Electronic Size Analysis of Subsieve Particles by Flowing Through a Small Liquid Resistor. Paper in STP 234, Am. Soc. Test. Mater., Philadelphia, PA, 1959, pp. 245-255.

20. Cashdollar, K. L., and M. Hertzberg. 20-L Explosibility Test Chamber for Dusts and Gases. Rev. Sci. Instrum., v. 56, 1985, pp. 596-602.

21. Conti, R. S., K. L. Cashdollar, and I. Liebman. Improved Optical Dust Probe for Monitoring Dust Explosions. Rev. Sci. Instrum., v. 53, 1982, pp. 311-313.

22. Richmond, J. K., M. J. Sapko, and L. F. Miller. Fire and Explosion Properties of Oil Shale. BuMines RI 8726, 1982, 39 pp.

23. Staff, Bureau of Mines. Fire and Explosion Hazards of Oil Shale. BuMines RI 9281, 1989, 63 pp.

APPENDIX A.—DETAILED MACHINE DRAWINGS AND CONSTRUCTION PROCEDURES FOR 1.2-L FURNACE

CONSTRUCTION PROCEDURES FOR U.S. BUREAU OF MINES 1.2-L FURNACE

A. Fabricating and curing combustion tube (fig. A-1)

1. Using a diamond-bladed saw, cut 3 in[1] off one 6-in length (4-in OD) of magnesium aluminum silicate ceramic tube that has one closed hemispherical end and one end open (COE). Two 6 in lengths of magnesium aluminum silicate are needed.

2. Cut a 3/4-in long sleeve from a 4-1/2-in OD magnesium aluminum silicate ceramic tube that is open at both ends (OBE). Attach the 3-in section and the 6-in section with this sleeve, thereby producing a 9-in combustion tube that is now closed on the top and bottom.

3. Drill four (3/16-in OD) holes 90° apart, 1 in above the center line of the 9-in combustion tube.

4. Drill and mate a 1-1/2-in OD magnesium aluminum silicate tube at the top and a 1-in OD magnesium aluminum silicate tube to the bottom of the 9-in combustion tube.

5. Thread or groove the resulting ceramic tube at a rate of 5 turns per inch, concentrating more threads towards the hemispherical ends.

6. Glaze all five pieces and cure at 1,300° C.

B. Heating element

1. Wrap combustion tube with approximately 384 in of 18-gauge Nichrome heater wire. (A 5-min epoxy used sparingly over the wire and the ceramic tube is very helpful.)

2. Coat assembly with high-temperature ceramic cement and cure at 300° C.

3. Wrap combustion tube with a layer of braided ceramic sleeving or high-temperature ceramic cloth, then coat the sleeving using ceramic cement and cure.

C. Outer shell

1. Assemble a sheet metal shell, approximately 12-in diameter by 12-in length.

2. To hold the chamber in place, cut two (12-in diam by 1/2-in) calcium silicate insulator board discs. Cut the appropriate size hole in the center of each disc, for the vent and dispersion ports.

3. Drill holes in the sheet metal shell for four sleeves and several screw holes to hold the top and bottom insulator boards in place. Four sleeves should be inserted into the outer metal shell. The four ceramic tubes (access ports) will pass through these sleeves, the sheet metal shell and onto the chamber where they are cemented in place.

D. Final assembly

1. Attach the bottom piece of calcium silicate insulator board to the sheet metal shell. Place the leftover 3-in length piece of magnesium aluminum silicate ceramic into the center of the shell and on top of the insulator board. Insert ceramic combustion chamber into sheet metal shell and onto the magnesium aluminum silicate ceramic tube. This tube is used to help support and align the combustion chamber.

2. Mount access ports (step C-3) and fill remaining volume between the wrapped chamber and its outer covering with the ceramic blanket insulation.

3. Make electrical connections and assemble the top calcium silicate insulator board.

4. Assemble the furnace collar (fig. A-2) to top portion of the combustion chamber, insert burst diaphragm with locking diaphragm holder.

5. Season the furnace. This is accomplished by heating the furnace in 50° C increments to 1,000° C over an 8-h period, in the confines of a fume hood.

E. Furnace control

1. A 12.5-mil Chromel-Alumel thermocouple located at the wall of the chamber controls the furnace temperature.

2. Electrical power - 110 VAC at 20 amps.

F. Dust disperser unit for 1.2-L furnace (fig. A-3).

[1]Dimensions are given in inches (in). To convert to centimeters, multiply by 2.54.

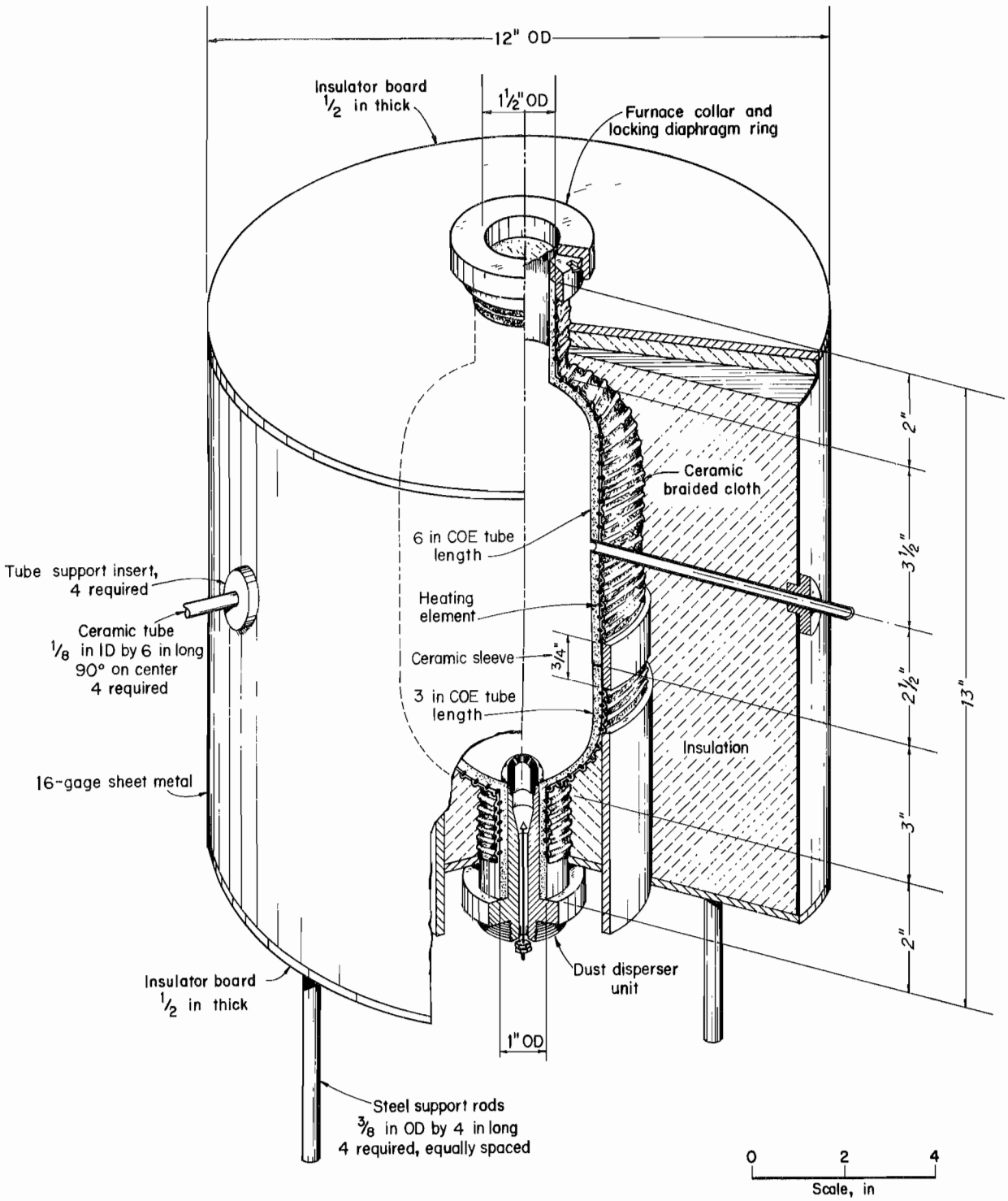

Figure A-1.—Assembly of 1.2-L furnace.

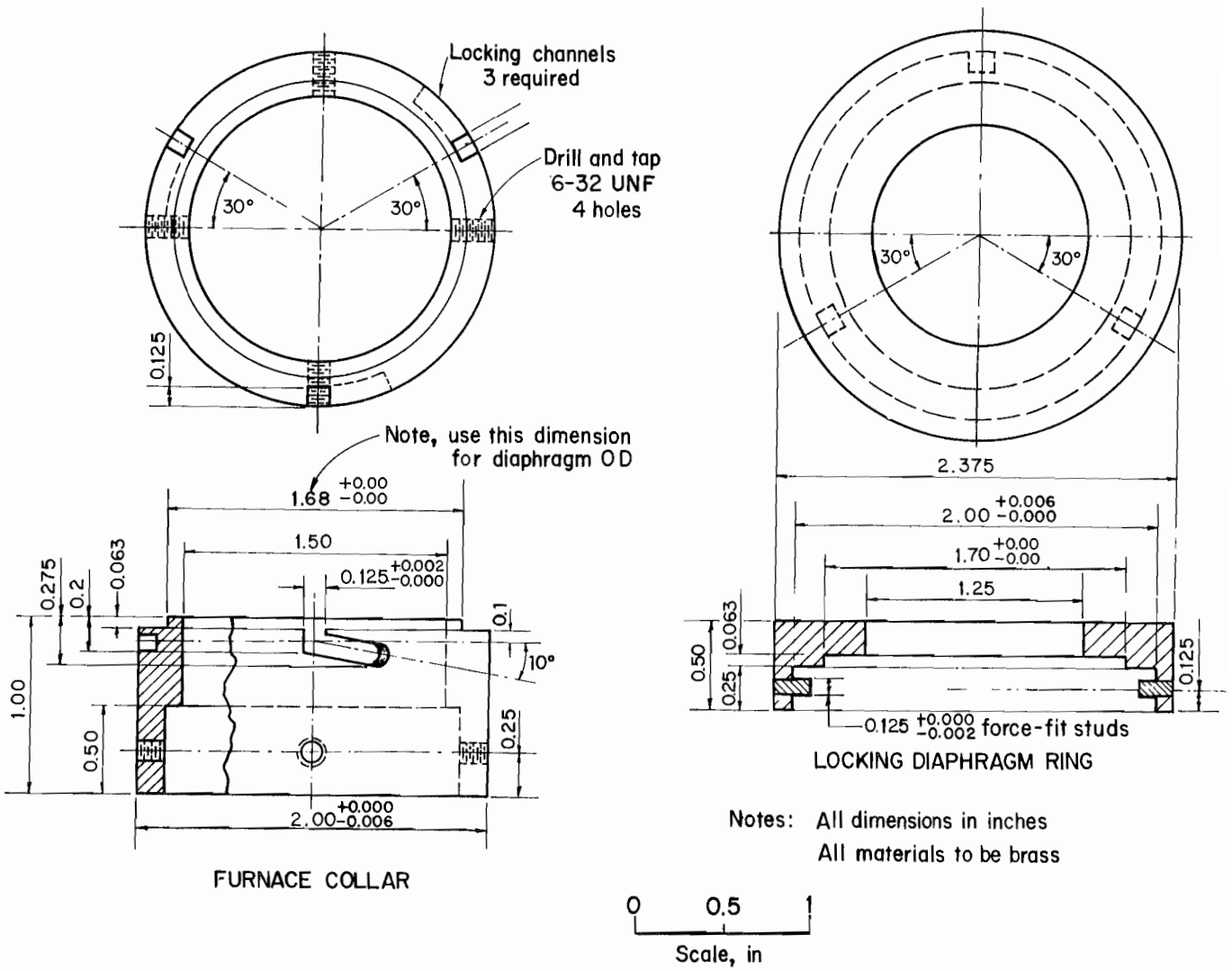

Figure A-2.—Collar and locking diaphragm ring for 1.2-L furnace.

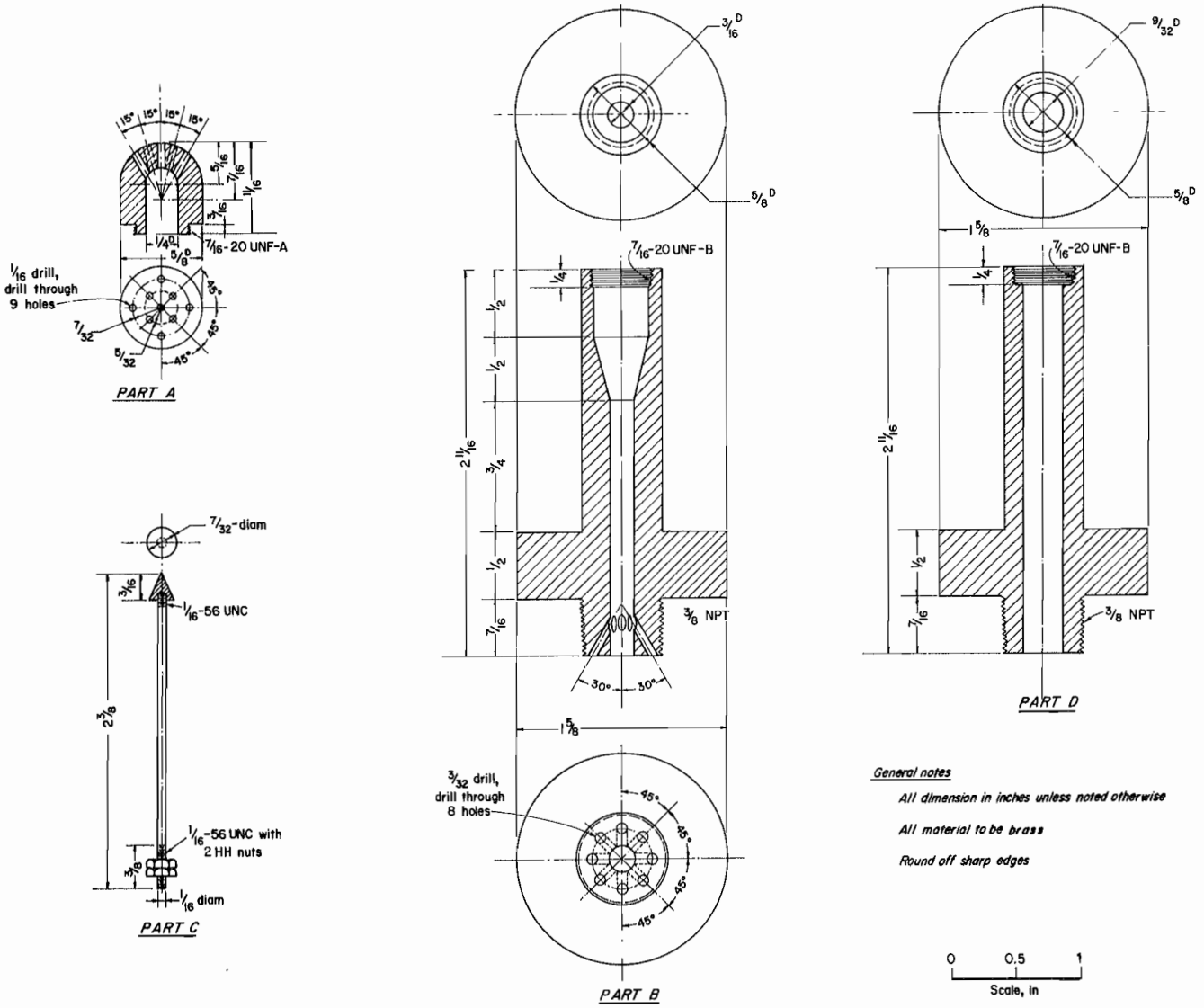

Figure A-3.--Dust disperser unit for 1.2-L furnace.

APPENDIX B.—DETAILED MACHINE DRAWINGS AND CONSTRUCTION PROCEDURES FOR 6.8-L FURNACE

CONSTRUCTION PROCEDURES FOR U.S. BUREAU OF MINES 6.8-L FURNACE

A. Fabricating and curing combustion tube (figs. B-1 - B-2)

1. Using a diamond-bladed saw, cut 1-in off a 8-in (7-7/8-in O.D.) length of magnesium aluminum silicate ceramic tube COE, and 2-7/8 inches off the other 8-in tube COE.

2. Attach the 7-in section and the 5-1/8-in section, thereby producing a 12-1/8-in combustion tube that is now closed on the top and bottom.

3. Drill six (0.380-in OD) holes 90° apart, 2-1/2-in above the connection joint of the 12-1/8-in combustion tube.

4. Using a diamond-bladed saw, cut a 2-1/2-in long piece of 1-1/2-in OD magnesium aluminum silicate ceramic tube and a 2-7/8-in section of 3-in OD magnesium aluminum silicate ceramic tube.

5. Drill and mate a 1-1/2-in OD magnesium aluminum silicate ceramic tube at the bottom, and drill and mate the 3-in OD magnesium aluminum silicate ceramic tube to the top of the 12-1/8-in combustion tube.

6. Thread or groove the resulting magnesium aluminum silicate ceramic tube at a rate of 5 turns per inch, concentrating more threads towards the hemispherical ends.

7. Glaze all four pieces and cure at 1,300° C.

B. Heating element

1. Wrap the combustion tube with approximately 1,600 in of 12-gauge Nichrome heater wire. (A 5-min epoxy used sparingly over the wire and ceramic tube is very helpful.)

2. Coat assembly with high-temperature ceramic cement and cure to the cement's specifications.

3. Wrap combustion tube with a layer of braided ceramic sleeving or high-temperature ceramic cloth, then coat the sleeving with cement and cure.

C. Outer shell

1. Assemble a sheet metal shell, approximately 18-in diameter by 16-in length.

2. To hold the chamber in place, cut two (18-in diam by 1/2-in) calcium silicate insulator board discs. Cut the appropriate size hole in the center of each disc, for the vent and dispersion ports.

3. Drill holes in the sheet metal shell for six Teflon fluorocarbon polymer (polytetrafluoroethylene) sleeves and several screw holes to hold the top and bottom insulator boards in place. Six Teflon fluorocarbon polymer sleeves (used for heat expansion) should be inserted into the outer metal shell. The six ceramic tubes (access ports 3/8-in OD) will pass through these sleeves, the sheet metal shell and to the chamber where they are cemented into place.

D. Final assembly

1. Attach the bottom piece of calcium silicate insulator board to the sheet metal shell. Place the 6-in-long tube OBE (7-7/8-in OD) into the center of the shell and on top of the insulator board. Insert ceramic combustion chamber into sheet metal shell and onto the 7-7/8-in OD tube. This tube is used to help support and align the combustion chamber.

2. Mount access ports (step C-3) and fill remaining volume between the wrapped chamber and the sheet metal shell with the ceramic blanket insulation.

3. Make electrical connections and assemble the top calcium silicate insulator board disc.

4. Assemble the furnace collar (fig. B-3) to top portion of the combustion chamber, insert quartz window with ceramic washers and tighten with locking ring.

5. Season the furnace. This is accomplished by heating the furnace in 50° C increments to 1,000° C over an 8-h period.

E. Furnace control

1. Furnace controller - current control.

2. A 12.5-mil Chromel-Alumel thermocouple located at the wall of the chamber controls the furnace temperature.

3. Electrical power - 220 VAC at 20 amps.

F. Dust disperser for 6.8-L ignitability furnace (fig. B-4).

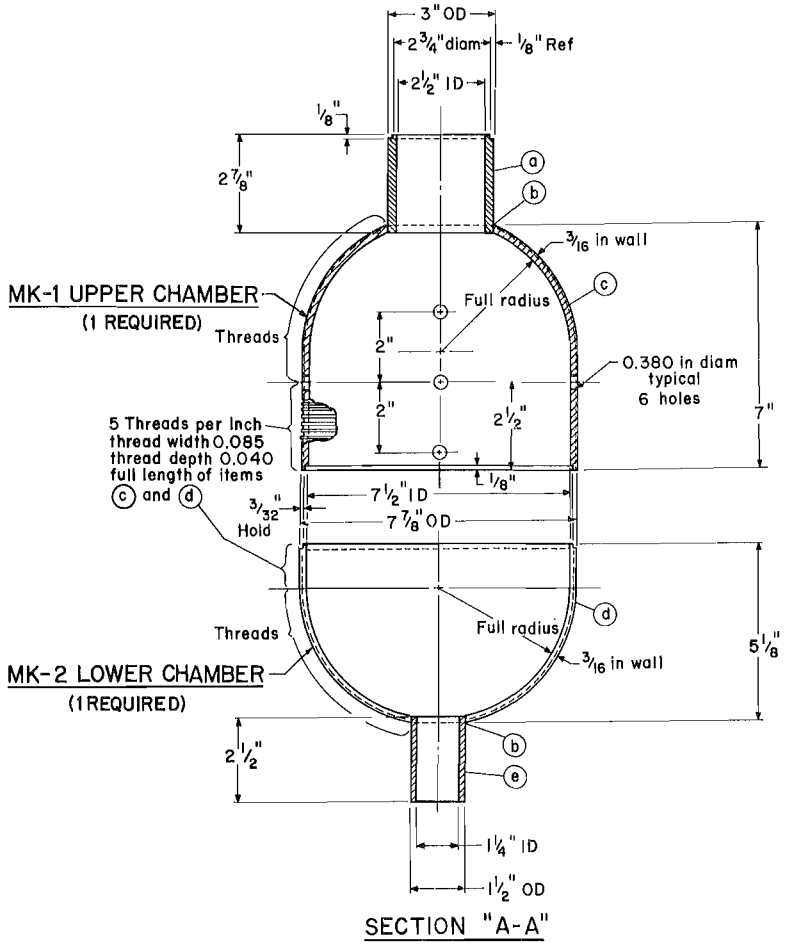

ITEM	QTY MK-1	QTY MK-2	NAME	DESCRIPTION
a	1	—	Tube	3" OD X 2 7/8" ID Long Ceramic
b	AR	AR	Cement	High Temperature Cement
c	1	—	Chamber	7 7/8" OD X 7 1/2" ID X 7" Long Ceramic
d	—	1	Chamber	7 7/8" OD X 7 1/2" ID X 5 1/8" Long Ceramic
e	—	1	Tube	1 1/2" OD X 1 1/4" ID X 2 1/2" Long Ceramic

NOTES:
1. Items (a), (c), (d), & (e), to be modified as shown
2. AR- as required

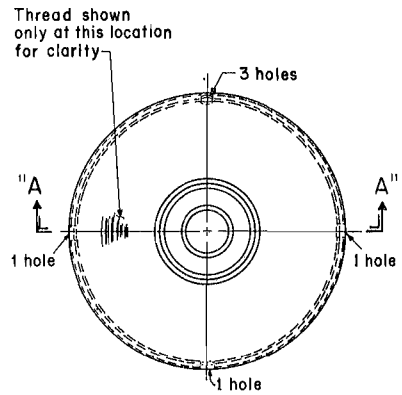

MK-3 FINAL ASSEMBLY

Figure B-1.—Combustion chamber for 6.8-L furnace.

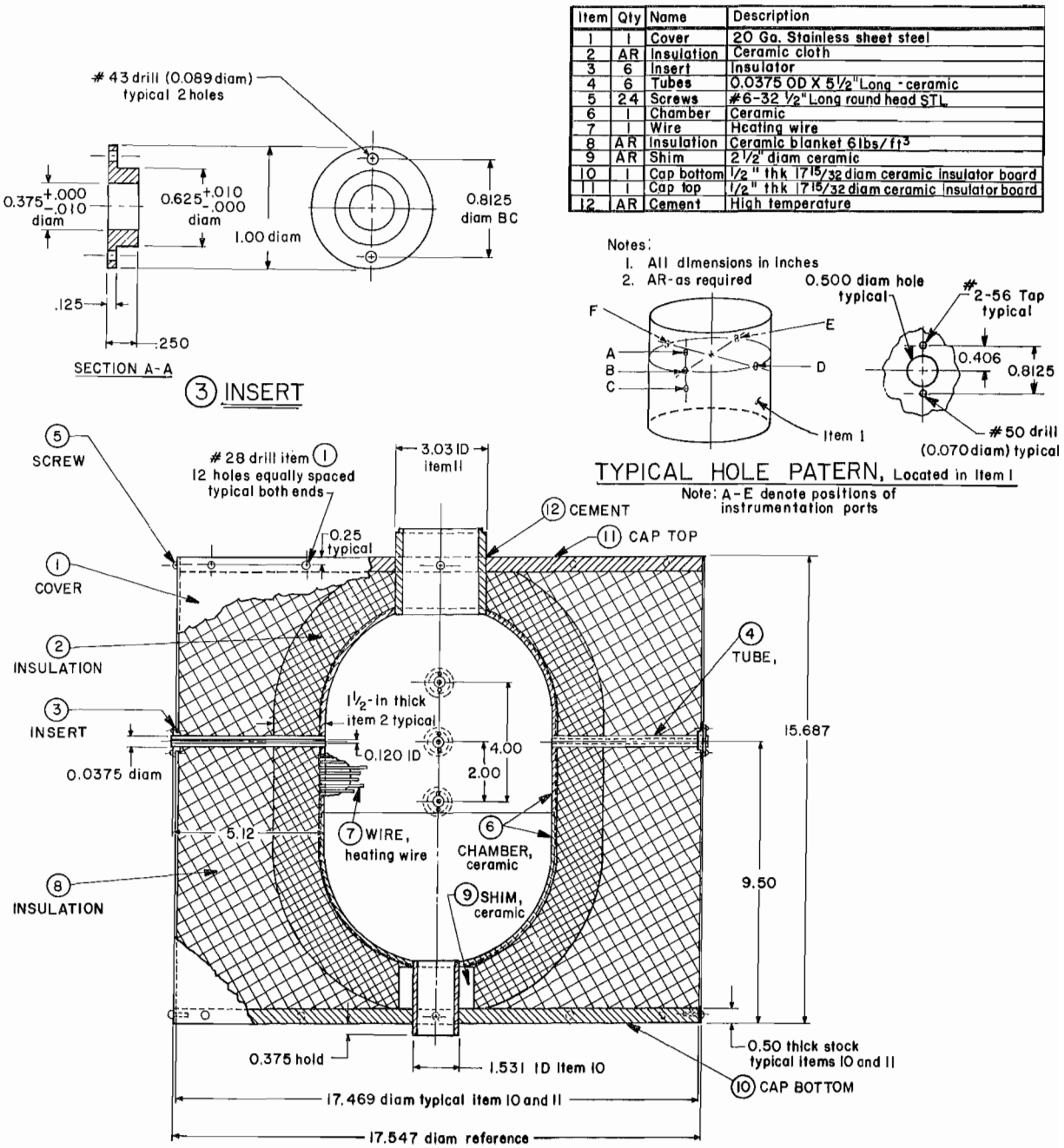

Item	Qty	Name	Description
1	1	Cover	20 Ga. Stainless sheet steel
2	AR	Insulation	Ceramic cloth
3	6	Insert	Insulator
4	6	Tubes	0.0375 OD X 5½" Long - ceramic
5	24	Screws	#6-32 ½" Long round head STL
6	1	Chamber	Ceramic
7	1	Wire	Heating wire
8	AR	Insulation	Ceramic blanket 6 lbs/ft³
9	AR	Shim	2½" diam ceramic
10	1	Cap bottom	½" thk 1 7 15/32 diam ceramic insulator board
11	1	Cap top	½" thk 1 7 15/32 diam ceramic insulator board
12	AR	Cement	High temperature

MK-1 FURNACE ASSEMBLY

Figure B-2.—6.8-L ignitability furnace.

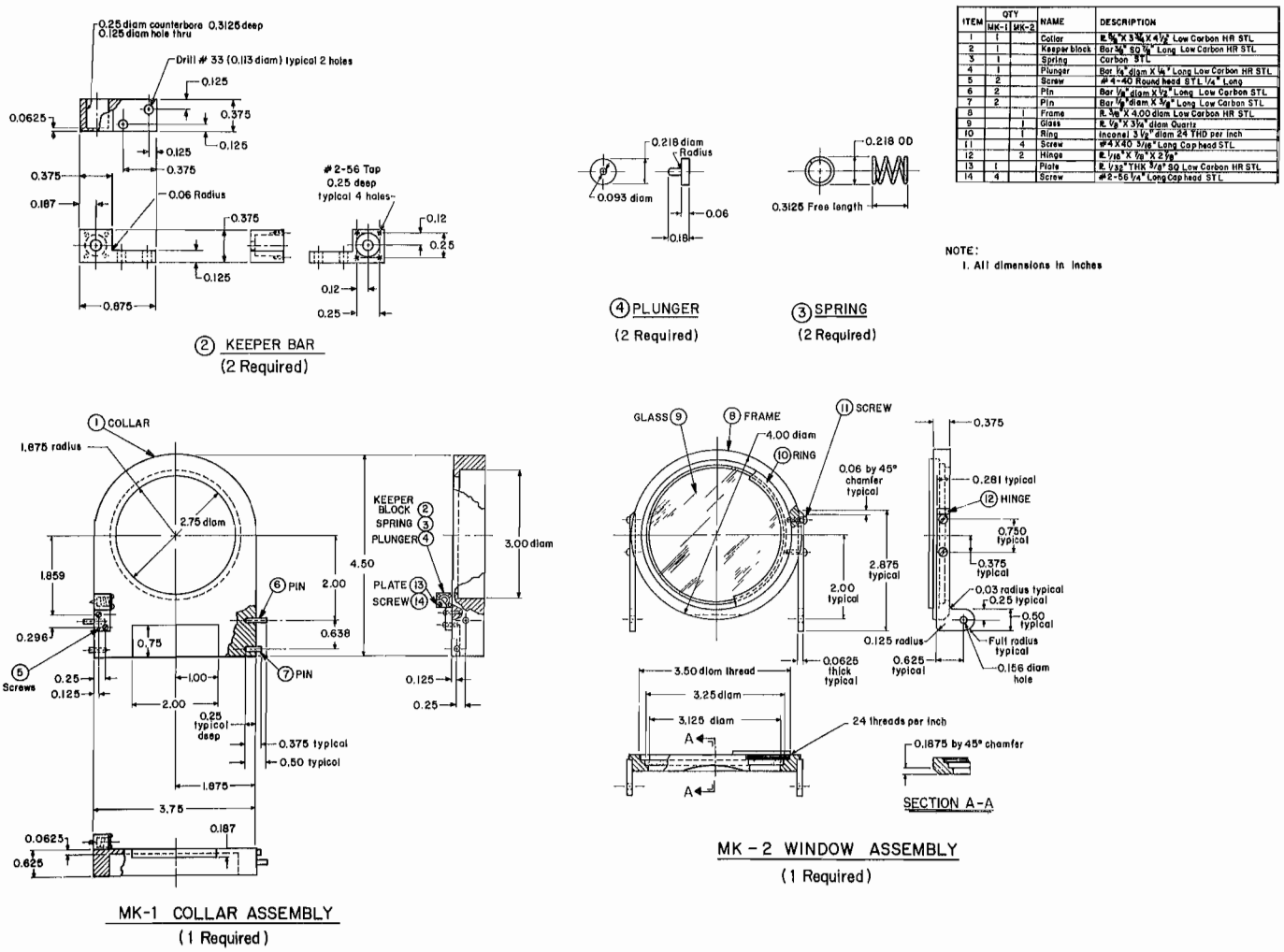

ITEM	QTY MK-1	QTY MK-2	NAME	DESCRIPTION
1	1		Collar	R. 5/8" X 3 3/4 X 4 1/2" Low Carbon HR STL
2	1		Keeper block	Bar 3/4" SQ 7/8" Long Low Carbon HR STL
3	1		Spring	Carbon STL
4	1		Plunger	Bar 1/4" diam X 1 1/4" Long Low Carbon HR STL
5	2		Screw	#4-40 Round head STL 1/4" Long
6	2		Pin	Bar 1/8" diam X 1/2" Long Low Carbon STL
7	2		Pin	Bar 1/8" diam X 5/8" Long Low Carbon STL
8		1	Frame	R. 3/8" X 4.00 diam Low Carbon HR STL
9		1	Glass	R. 1/8" X 3 1/4" diam Quartz
10		1	Ring	Inconel 3 1/2" diam 24 THD per inch
11		4	Screw	#4 X 40 5/16" Long Cap head STL
12		2	Hinge	R. 1/16" X 7/8" X 2 1/8"
13	1		Plate	R. 1/32" THK 3/4" SQ Low Carbon HR STL
14	4		Screw	#2-56 1/4" Long Cap head STL

Figure B-3.—Door assembly and details of 6.8-L ignitability furnace.

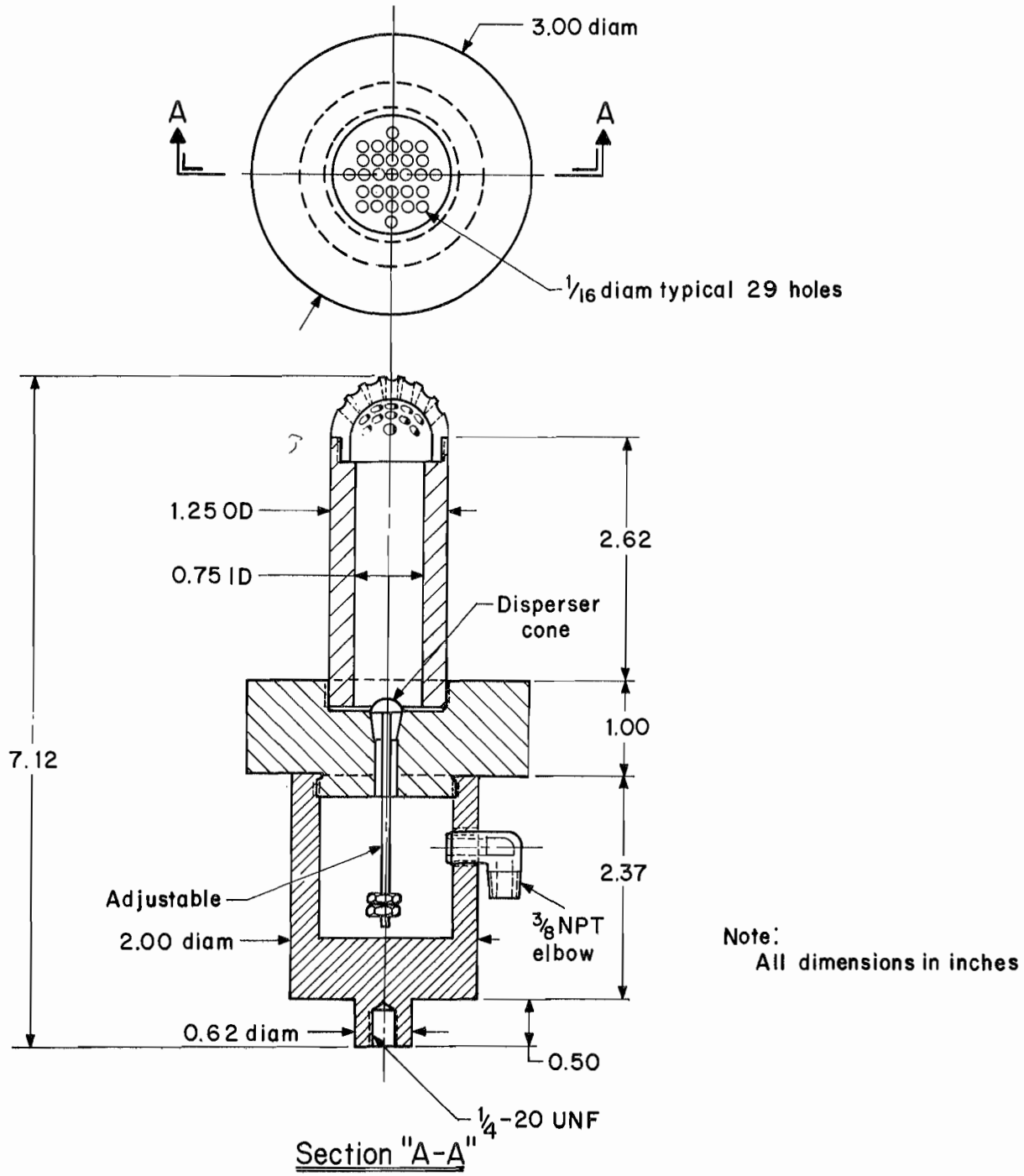

Figure B-4.—Outline dust disperser of 6.8-L ignitability furnace.

INT.BU.OF MINES,PGH.,PA 29764

*U.S.G.P.O.: 1993--709-088/80014